EXPERIMENTAL STUDY OF THE EFFECTS OF THERMALLY CONDUCTIVE MICROPOROUS COATINGS ON LOW HEAT FLUX POOL AND FLOW BOILING

by

MATTHEW MLCAK

Presented to the Faculty of the Graduate School of

The University of Texas at Arlington in Partial Fulfillment

Of the Requirements for the Degree of

MASTER OF SCIENCE IN MECHANICAL ENGINEERING

THE UNIVERSITY OF TEXAS AT ARLINGTON

AUGUST 2010

ACKNOWLEDGEMENTS

I would like to thank my family for all of their support and guidance throughout my life and collegiate career. I would like to specially thank my wife for all of her support and motivation in my graduate studies. I would like to thank my lab mates who have graduated and continue their studies at UTA for their help with procedures and lab guidance. I also want to offer thanks to Dr. Amaya for his help and support with writing and editing my thesis and all the long meetings that he participated in.

My final thanks goes out to Dr. You for allowing me to study in his lab and under his close guidance. He has offered his expertise and insight throughout my time at UTA.

June 3, 2010

ABSTRACT

EXPERIMENTAL STUDY OF THE EFFECTS OF THERMALLY CONDUCTIVE MICROPOROUS COATINGS ON LOW HEAT FLUX POOL AND FLOW BOILING

Matthew Mlcak M.S.

The University of Texas at Arlington, 2010

Supervising Professor: Seung Mun You

This study examines the effect of the Thermally Conductive Micro-porous Coating (TCMC) developed at the University of Texas at Arlington, on an extended length heater in flow boiling. The study was performed with application to heat transfer in a tankless hot water heater in mind. The coating is composed of copper particles of micron size soldered to each other and to the substrate. The optimal TCMC (75μm particles with a thickness of 425μm±25μm) was first determined from pool boiling tests. The coating was then tested in flow boiling utilizing tap water as the working fluid at two different levels of subcooling, 80°C and 50°C, and at three different flow rates, 0.25, 0.50, and 1.00lpm. The gassy-subcooled flow boiling tests showed the appearance of a partially developed boiling regime and stationary gas-vapor bubbles. The bubbles eventually blanketed the surface of the heater and influenced heat transfer as significantly as the coating. The coating was detrimental or offered no benefits in this regime. The flow boiling tests still showed that in fully developed boiling, the coating enhanced heat transfer relative to the plain heater. This enhancement could be translated into a potential reduction of heater transfer area of up to ~18%, or a lowering of the surface temperature of the heater relative to the plain heater by up to 10°C.

TABLE OF CONTENTS

ACKNOWLEDGEMENTS iii

ABSTRACT iv

LIST OF ILLUSTRATIONS viii

LIST OF TABLES xi

NOMENCLATURE xii

Chapter Page

1. INTRODUCTION 1

1.1 Literature Review 1

1.1.1 Pool Boiling 1

1.1.2 Current Enhancement Techniques in Pool Boiling 3

1.1.3 Flow Boiling 4

1.1.4 Current Enhancement Techniques in Flow Boiling 5

1.2 Project Motivation 6

1.3 Project Objectives 7

2. EXPERIMENTAL TEST SETUP AND PROCEDURES 8

2.1 Pool Boiling Test Setup 8

2.1.1 Boiling Vessel 8

2.1.2 Pool Boiling Heater 10

2.2 Flow Boiling Test Setup 11

2.2.1 Flow Boiling Test Section 11
2.2.2 Procedure for Making Heaters 13
2.2.3 Procedure for Making TCMC 13
2.3 Procedure For Making Extended Surface Coatings 15
2.4 Procedure for Cleaning TCMC 15
2.5 Experimental Test Procedures 16
2.6 Uncertainty Analysis 16
3. RESULTS AND DISCUSSION 17
3.1 Pool Boiling 18
3.1.1 References Curves 18
3.1.2 Pool Boiling-75µm Particles 19
3.1.3 Pool Boiling-120µm Particles 21
3.1.4 Comparison of Optimal 75µm and 120µm Particles 24
3.2 Flow Boiling 26
3.2.1 Effect of Silicone Contamination 27
3.2.2 Flow Boiling Parameters 31
3.2.3 Subcooling at 80°C 32
3.2.4 Subcooling at 50°C 40
3.2.5 Comparison of Flow Boiling to Pool Boiling 43
3.2.6 Enhancement Through Heater Area Reduction 44
4. CONCLUSIONS AND RECOMMENDATIONS 47
4.1 Pool Boiling 47

4.2 Flow Boiling 47

4.3 Recommendations 48

APPENDIX

A. PICTORAL ANALYSIS OF STATIONARY BUBBLE PHENOMENON 50

REFERENCES 55

BIOGRAPHICAL INFORMATION 59

LIST OF ILLUSTRATIONS

Figure Page

1.1 Standard boiling curve [13] 2

1.2 Enhancement of BHT and CHF in pool boiling 3

1.3 Flow boiling regimes [16] 4

1.4 Sample cross-section of microchannel [21] 6

2.1 CAD representation of pool boiling test section 9

2.2 1cm x 1cm heater setup for (a) final heater and (b) exploded view 10

2.3 2cm x 2cm heater setup for (a) final heater and (b) exploded view 11

2.4 Flow boiling test loop 12

2.5 Exploded view of flow boiling test section 12

3.1 Comparison of plain copper heaters performance to Rohsenow correlation 19

3.2 Pool boiling results for 75µm particle coatings at various thicknesses 20

3.3 Effect of coating thickness on heat transfer coefficient for 75µm particles 21

3.4 Pool boiling results for 120µm particle coatings at various thicknesses 22

3.5 Effect of coating thickness on heat transfer coefficient for 120µm particles 23

3.6 Comparison of optimized coatings 25

3.7 Repeatability of coating generation technique 26

3.8 Cross section illustration of (a) clean TCMC and (b) perimeter contamination on TCMC 27

3.9 Microscope images of (a) full view clean coating, (b) full view silicone contaminated coating, (c) close up of edge of clean coating, and (d) close up of edge of silicone contaminated coating 28

3.10 Effect of silicone contamination on coated surface in subcooled test 30

3.11 Boiling curve adjusted for correct area 31

3.12 Copper block with dimensions 32

3.13 Flow boiling curve for plain and coated at 0.25lpm and 80°C subcooled 34

3.14 Bubbles on plain surface between (a) 6W/cm^2 - 8W/cm^2, (b) 10W/cm^2 - 12W/cm^2, (c) 12W/cm^2 - 14W/cm^2, (d) 14W/cm^2 - 16W/cm^2, and (e) 16W/cm^2 - 18W/cm^2 35

3.15 Bubbles on coated surface between (a) 2W/cm^2 - 4W/cm^2, (b) 4W/cm^2 - 6W/cm^2, (c) 6W/cm^2 - 8W/cm^2, (d) 8W/cm^2 - 10W/cm^2, and (e) 12W/cm^2 - 14W/cm^2 37

3.16 Effect of flow rate at 80°C subcooling for coated and plain heaters 39

3.17 3-D Plot of heat transfer coefficient, heat flux, and flow rate for coated heater at 80°C subcooled 40

3.18 Effect of flow rate at 50°C subcooling for coated and plain heaters 42

3.19 3-D Plot of heat transfer coefficient, heat flux, and flow rate for coated heater at 50°C subcooled 43

3.20 Comparison of gassy-subcooled flow boiling to gassy-subcooled pool boiling over coated heaters 44

3.21 Reduction in area 45

A.1 Flow boiling curves of plain and coated heaters 51

A.2 Number of stationary bubbles over plain heater (left) and over coated heater (right) at 14W/cm^2 51

A.3 Flow boiling curves for repeated tests over the same plain heater 52

A.4 Number of stationary bubbles of 1st plain heater run (left) and 2nd plain heater run (right) at 12W/cm^2 52

A.5 Fouling on the plain heater after ~10 tests in tap water 53

A.6 Flow boiling curve of 1st coated heater run and 2nd coated heater run 53

A.7 Number of stationary bubbles of 1st coated heater run (left) and 2nd coated heater run (right) at 12W/cm^2 54

LIST OF TABLES

Table Page

2.1 TCMC cleaning protocol 15

3.1 Pool boiling parameters 17

3.2 Flow boiling parameters 17

3.3 Values of surface parameter, C_{sf}, in Rohsenow correlation [16] for various combinations of metals and liquids 18

3.4 Flow boiling parameters and resulting flow values 32

NOMENCLATURE

BHT	boiling heat transfer
CHF	critical heat flux
DNB	departure from nucleate boiling
FDB	fully developed boiling
TCMC	thermally conductive micro-porous coating
C_p	specific heat (J/kg K)
h_{LG}	latent heat vaporization (kJ/kg)
P_r	Prandtl number
h	heat transfer coefficient
q”	heat flux (W/cm^2)
Q	power (Watt)
A	area (cm^2)
T	temperature (°C)
ΔT_{sat}	surface temperature – saturation temperature (°C)

GREEK SYMBOLS

μ_L	liquid dynamic viscosity (kg/m s)
σ	surface tension (N/m)
ρ_L	density of liquid (kg/m^3)
ρ_G	density of gas (kg/m^3)

SUBSCRIPTS

c	coated
p	plain
sur	surface
sat	saturated
inlet	inlet
1	location 1
3	location 3
L	liquid
v	vapor

CHAPTER 1

INTRODUCTION

In today's society, energy consumption is increasing and energy savings are becoming more important and essential. Improvements in the efficiency of heat transfer equipment have been seen in fields ranging from tankless hot water heaters in home applications to desalination systems to provide drinking water. The potential improvements in a tankless hot water heater are to reduce the overall heated length to save space and to reduce the heater surface temperature to extend the life of the heater. Microstructures [1, 2] and particularly thermally conductive micro-porous coatings (TCMC) [3] have increased the critical heat flux (CHF) and the boiling heat transfer (BHT) of working fluids in flow boiling applications. TCMC was developed by researchers at The University of Texas at Arlington [4] and consists of copper particles and solder that are combined and affixed to a heater surface to produce porous structures with internal microcavities.

1.1 Literature Review

1.1.1 Pool Boiling

Pool boiling is the boiling of a stationary pool of water with a heater or a heated test surface. This technique is used to observe both single-phase and two-phase heat transfer. In two-phase heat transfer, the pool boiling testing scheme allows for the observation of the onset of boiling, the nucleate boiling regime, and the departure from nucleate boiling. A typical saturated boiling curve can be seen in Figure 1.1. This curve shows the wall superheat, defined as the surface temperature minus the bulk fluid temperature, on the x-axis and the heat flux on the y-axis. The curve is generated experimentally by incrementing the heat flux and

measuring the corresponding wall superheat. The natural convection region is defined as the location where no phase change yet occurs. The discrete bubble region is where the heat transfer mode transitions from natural convection to the beginning of phase change and is the beginning of the nucleate boiling regime. The vapor mushroom region occurs after the first transition region and is where the bubble size begins to increase. The second transition region is where the bubble size begins to grow so large that the vapor blankets the entire surface. This process is described as departure from nucleate boiling (DNB) and leads to CHF of the surface. During the CHF, the temperature of the heated surface spikes. The CHF phenomenon has been studied with many different heater materials, surface enhancements [5-8], fluids [9], and applications utilizing nanofluids [10-12]. An increase in the CHF is described as enhancement in CHF. Enhancement in BHT is represented by a shift to the left of the pool boiling curve in the nucleate boiling regime. The enhancements in BHT and CHF in terms of the pool boiling curve are illustrated in Figure 1.2.

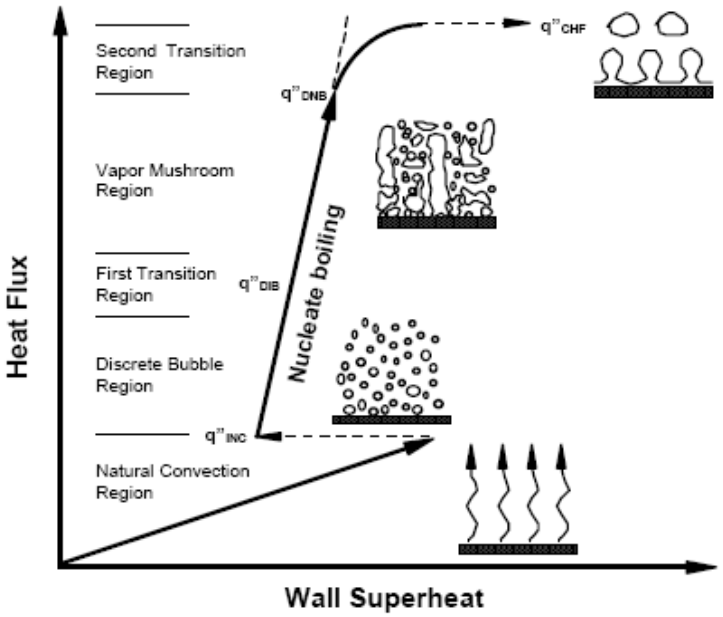

Figure 1.1 Standard boiling curve [13]

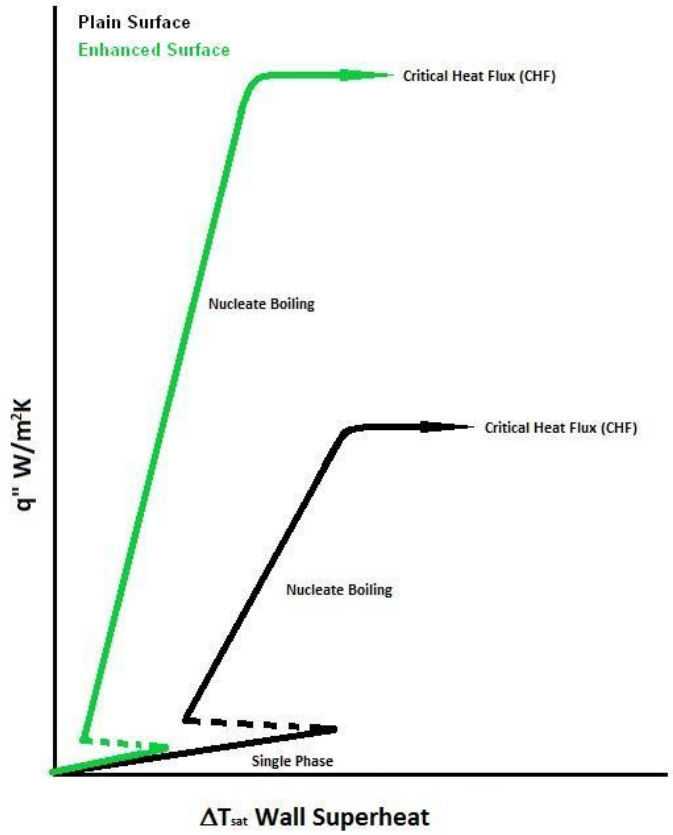

Figure 1.2 Enhancement of BHT and CHF in pool boiling

1.1.2 Current Enhancement Techniques in Pool Boiling

It is known that modifying the surface of a heater will change the onset of nucleate boiling and the surface temperature during nucleate boiling, with certain modifications lowering both. These modifications are highly advantageous since the two-phase regime allows for greater dissipation of heat than single-phase natural convection. The initial attempt to enhance the surface of a heater was to incorporate patterns on the surface either by roughening with sand paper or by machining. These treatments increased the surface area and locations for boiling to initiate. The effect of machined surfaces on nucleate boiling was previously studied by Das et al [7]. The University of Texas at Arlington has been a frontrunner in the research of

surface modification to enhance the BHT and CHF [14, 15]. TCMC has enhanced BHT and CHF with FC-72 as the working fluid [3]. The increase in CHF is very important in applications such as cooling of small electronic packages with very high heat flux. The early onset of nucleate boiling and the increased CHF allows for a lower surface temperature at increasing heat flux ranges.

1.1.3 Flow Boiling

Boiling of a fluid that is moving through a pipe or conduit is called flow boiling. Multiple heat transfer regimes can be present when a fluid moves through a heated conduit. The heated length of the conduit influences how many regimes can be present. The regimes that are often found in flow boiling are illustrated in Figure 1.3.

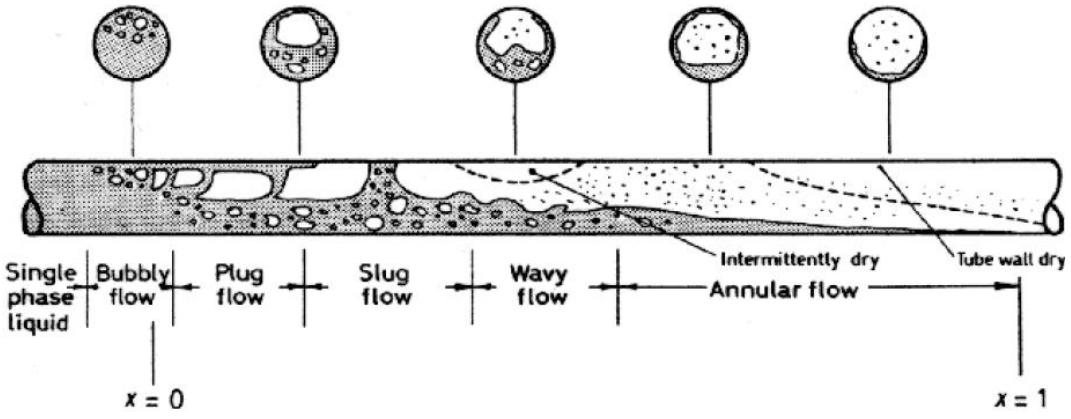

Figure 1.3 Flow boiling regimes [16]

The most common flow boiling configurations are flow through horizontal and vertical tubes [17] and tubes with various shapes ranging from round to square, and other less common shapes. When flow boiling occurs in a horizontal tube, gravity causes the liquid to stay at the bottom periphery of the tube and the gas at the top as illustrated in Figure 1.3. CHF in flow boiling is the heat flux that leads to dryout but is not seen if the heated length is not sufficiently

long for the given heat flux. Dryout is illustrated in the far right of Figure 1.3. An example of where dryout can pose a problem is when the wall is heated by an electronic component or electric heater where failure of the component may occur from the high surface temperature at the CHF. An example of where dryout can be useful is in the evaporator of an air conditioner utilizing the reverse Rankine cycle. Dryout is necessary in this example because the refrigerant must be all gas when leaving the evaporator since the compressor can only compress and propel a gas. Of the regimes shown in Figure 1.3, only the single-phase liquid and bubbly flows are present in a tankless hot water heater. Therefore this study will focus on low heat flux applications where only single-phase and bubbly flow regimes are present.

1.1.4 Current Enhancement Techniques in Flow Boiling

Flow boiling is becoming more important as the heat fluxes that must be dissipated are increasing. An example is a supercomputer where the chip size is rapidly decreasing and the power consumption is rapidly increasing, producing extremely high heat fluxes. It is becoming more popular to use flow boiling due to its increased heat transfer coefficient and the increased CHF. Surface roughening is commonly employed in industrial applications such as HVAC or heat exchangers and is called rifling. The effects of rifling or spirally corrugated tubes on heat transfer have been studied [18]. The greatest effect of this type of enhancement is to induce turbulent flow which in turn increases the heat transfer coefficient. Another type of enhancement is to increase the heat transfer area through the use of fins [19, 20]. Another way to increase the heat transfer coefficient is by flow through microchannels. The very small hydraulic diameter in the microchannel causes the velocity and heat transfer coefficient to increase. Microchannels have been shown to increase the CHF by Lee and Mudawar [21]. In their study, the width and height of the microchannel ranged from ~120-250μm and ~300-1000μm respectively. The microchannels were oriented along the top of the copper heater in the direction of flow (Figure 1.4). Combinations of different working fluids and enhanced geometries have been used to give the best heat transfer performance enhancement [2, 22, 23]. TCMC has also been used for the

enhancement of flow boiling with FC-72 [3] as the working fluid. TCMC benefits flow boiling in nearly the same way as in pool boiling. The coating increases the number of nucleation sites which lowers the onset of nucleate boiling and the wall superheats [13].

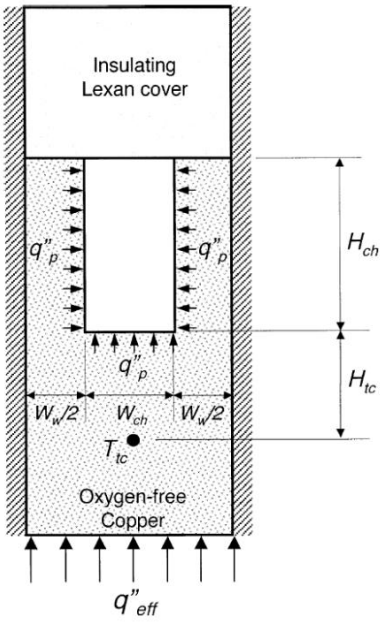

Figure 1.4 Sample cross-section of microchannel [21]

1.2 Project Motivation

Tankless hot water heaters are increasing in popularity because of the energy savings that they offer. Unlike conventional hot water heaters where a reservoir of water is maintained hot, energy is saved in tankless hot water heaters because the water is heated only on demand. The objective of this study is to evaluate the effects of TCMC in a tankless water heater application. It is believed that TCMC can increase the heat transfer coefficient of a heater through the earlier onset of nucleate boiling and through an increase in nucleation sites. The increased heat transfer coefficient could allow for a reduction in the heated length required to provide a given heat transfer rate in the residential tankless water heater. Area savings could also be achieved through TCMC in the HVAC and heat exchanger industries, leading to more

compact air conditioning systems. These smaller systems would benefit the military and the automotive industry because space is a premium. Also TCMC could lower the wall superheat at a given heat flux extending the life of a tankless hot water heater.

1.3 Project Objectives

The primary objective of this experimental study is to discover the potential benefits of TCMC in low heat flux flow boiling situations. TCMC has been optimized for increasing the CHF and the BHT over the whole range of heat fluxes up to CHF, but it has not been optimized for the narrower, lower range (up to 20W/cm^2, discrete bubble region in Figure 1.1) seen in applications such as in the tankless hot water heater. Therefore, this research evaluates coatings at combinations of two particle sizes and various thicknesses in low heat flux flow boiling. First, pool boiling tests are conducted and evaluated to find the coating with the combination of particle size and coating thickness that maximizes BHT. Then, this coating is tested in flow boiling. The surface temperature is monitored and performance is characterized in terms of potential heated length reductions or temperature reductions.

CHAPTER 2

EXPERIMENTAL TEST SETUP AND PROCEDURES

2.1 Pool Boiling Test Setup

2.1.1 Boiling Vessel

The test section adopted has previously been used by other researchers in the Micro-Scale Heat Transfer Lab at The University of Texas at Arlington. The pool boiling apparatus can be seen in Figure 2.1 and consists of two aluminum plates with a thick walled cylinder of glass pressure fitted between them. The glass is a low expansion borosilicate composition produced by Corning Pyrex. The two aluminum plates are approximately 200mm in diameter and 20mm thick. The top plate incorporates sealed holes for the wires that supply power to the heater and for connecting the thermocouples to the Data Acquisition System (DAQ). This allows the system to remain sealed during degassing. Degassing is a process to remove the noncondensable gases that are present in a fluid below saturation temperature. This insures that the boiling test is performed on pure water alone. There is a hole for a cartridge heater for heating the fluid in order to maintain a set bulk temperature of the fluid. Another hole or port in the vessel is connected to a heat exchanger which is used as a condenser while the system is degassing. This eliminates the possibility that the system will lose water vapor during the course of the degassing process. The condenser allows the noncondensable gases, or air, to escape out of the system and the water vapor to condense and flow back into the vessel. Three thermocouples measure the water, vapor, and liquid temperature. Type-T thermocouples, temperature range of -185°C to 300°C with a tolerance of ±.5°C, are used. The metals of the Type-T thermocouple are copper and constantan. The thermocouples are made by soldering

the two tips of the metals together. A drain hole is provided in the bottom plate. The vessel is sealed using four threaded rods as seen in Figure 2.1

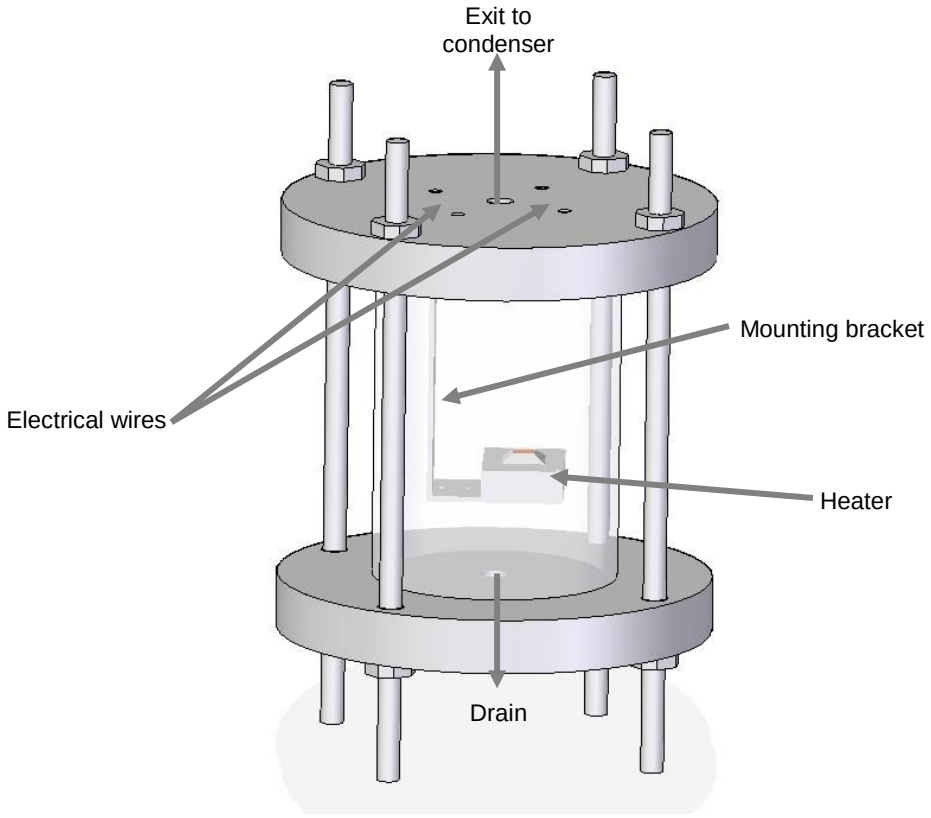

Figure 2.1 CAD representation of pool boiling test section

The nuts are tightened to insure that the two plates are applying enough pressure on the glass to seal the system. Rubber gaskets between the glass and metal ensure a good seal throughout the duration of the test. The glass tube offers a large amount of visibility at all angles. This enables the user to easily spot edge boiling or other undesirable scenarios so that the test can be stopped if necessary. The final piece of the vessel is an aluminum L-Bracket that holds the heater and maintains its orientation during the test.

2.1.2 Pool Boiling Heater

Two sizes of heaters, 1x1cm^2 and 2x2cm^2, and copper blocks were used depending on the variant of TCMC tested. The resistive heaters were produced by Thick Film Technologies. The 1cm x 1cm heater can be seen in Figure 2.2. The heater is a resistive element that measures exactly 1cm x 1cm and is 1mm thick. One side of the heater is silicon and has the resistive element embedded on it. The other side is metal for easy soldering of the heating element to the copper surface. The copper block for this heater set up is also 1cm x 1cm and has a thickness of 3mm. The copper block has a 1mm diameter hole drilled 1.5mm below the surface of the block to embed the thermocouple into the center of the heater. The exact position of the thermocouple is then known and can be used to calculate the surface temperature of the heated surface through 1-D conduction. Epoxy is then used to attach the heater setup to a lexan substrate. Lexan is used because of its low thermal conductivity and high temperature capabilities.

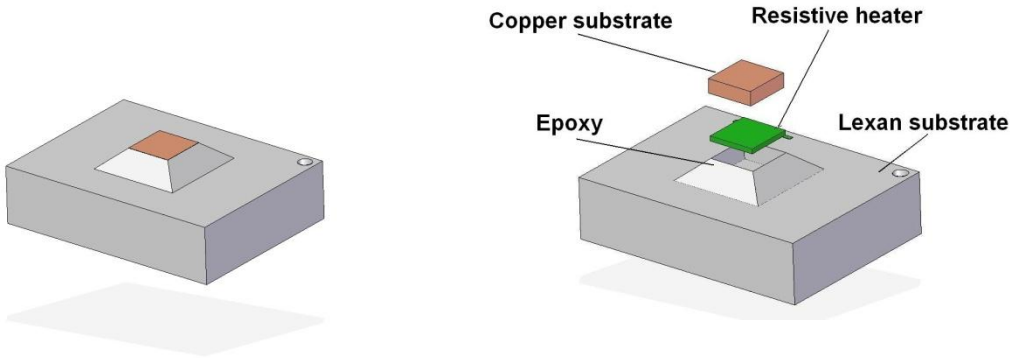

(a) (b)

Figure 2.2 1cm x 1cm heater setup for (a) final heater and (b) exploded view

The 2cm x 2cm heater is set up similarly to the 1cm x 1cm heater and can be seen in Figure 2.3. The heating element is resistive and made of silicon with the same features described for the 1cm x 1cm heater. The copper block is 2cm x 2cm and is 4mm thick. There is

a 1mm hole drilled 2mm below the surface in the center of the block for insertion of a thermocouple. The heater is attached to the lexan in the same way as described for the 1cm x 1cm heater.

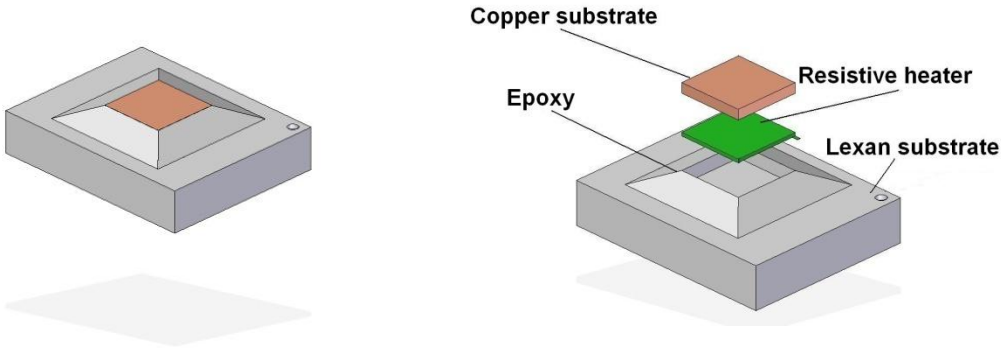

(a) (b)

Figure 2.3 2cm x 2cm heater setup for (a) final heater and (b) exploded view

2.2 Flow Boiling Test Setup

2.2.1 Flow Boiling Test Section

The flow boiling test section for this study is a closed loop system that consists of an isothermal bath, pump, flow meter, heated flow channel, and condenser. Figure 2.4 shows all of the flow boiling components. The pump is a constant displacement pump that has a control knob that precisely controls the flow rate. The flow rate is measured in real time and recorded at every power increment during the course of the test. The flow boiling test section has thermocouples at the inlet, outlet, and three heated surface locations. Figure 2.5 shows the heater test section. The portion of the copper block exposed to the flow is 25.4cm long and 1cm wide, giving a surface area of 25.4cm^2. Three thermocouples are located along the length of the heated surface with 6.35cm separating them and 6.35cm from the inlet to the first thermocouple and from the third thermocouple to the outlet. The block is heated using two cartridge heaters

that are inserted from each end of the copper block. The copper block has flanges located on the perimeter of the flow boiling area that seal the copper block against the lexan.

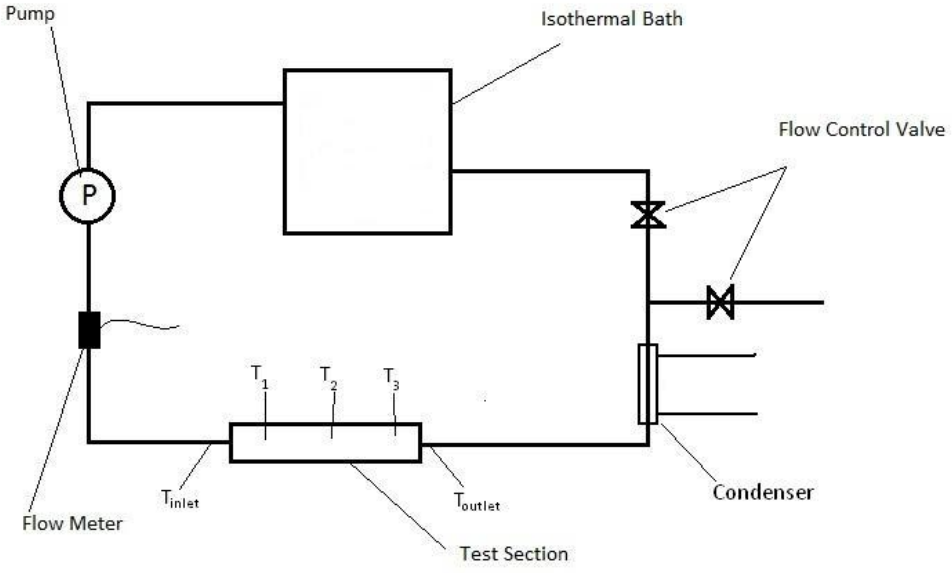

Figure 2.4 Flow boiling test loop

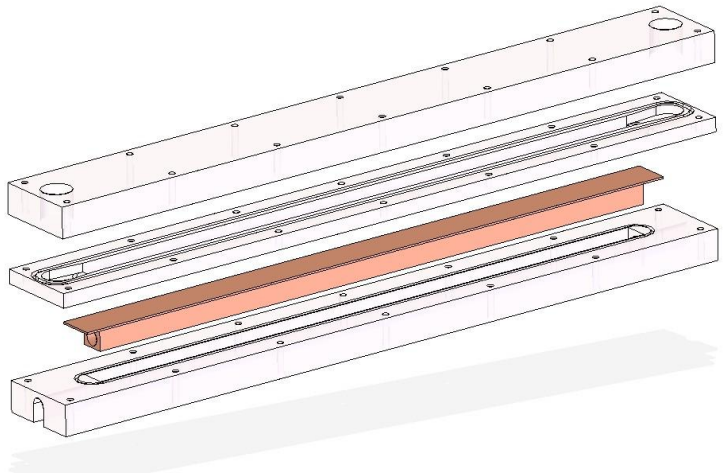

Figure 2.5 Exploded view of flow boiling test section

The flow meter used is an Omega 600 series and measures the flow rate based on the vane rpm. The isothermal bath maintains a precise inlet temperature through the duration of the test. The condenser is a copper coil that is submerged in water that is maintained at a very low temperature, allowing the heat added by the test section to be removed.

2.2.2 Procedure for Making Heaters

The following procedure is used for both sizes (1cm x 1cm, 2cm x 2cm) of the plain copper heaters and both sizes of the TCMC coated heaters. The heater and the copper block are soldered together using 60/40 (Tin/Lead) solder that melts at 190°C. A thin film of C-Flux that contains 95/5 (Tin/Antimony) is placed on the metal side of the heating element with a q-tip to prepare the surface for soldering. The heating element is then placed on a hot plate where the temperature can be precisely controlled. The heating element is heated to just above the solder melting temperature and the solder is melted on the metal side of the heating element. The copper block is placed upon the heating element and squared so that the heating element and the copper block are aligned. Solder is filled into the hole on the side of the copper block to prepare the hole for the thermocouple. The thermocouple is then inserted into the hole. Next the entire setup is quickly and carefully removed from the hot plate so as not to disturb the test surface, plain or coated. After the assembly cools down, it is attached to the lexan substrate using epoxy. The epoxy must be carefully applied to prevent edge boiling. Edge boiling can occur when the edges of a heater are not properly sealed. Water can get between the side of the heater and the epoxy which causes boiling to occur at this location before boiling initiates at the surface. This can cause erroneous results since the heated surface is larger than the intended size.

2.2.3 Procedure for Making TCMC

TCMC is a mixture of copper particles, solder, and alcohol. The solvent evaporates in the final coating. The procedure for making the coatings depended on the particle size. Two

particle sizes were used in this investigation, 75µm and 120µm particles. These values are the average size in a sample of particles that is captured between two meshes.

The preparation technique of the coating containing 75µm particles has been previously used in the Micro-Scale Heat Transfer Lab. The average coating thickness obtained by this technique is approximately 150µm thick. The coating is made from a mixture of copper particles and plumbing solder that are mixed in a ratio of two to one by weight. The mixture is then thinned with isopropyl alcohol. The alcohol is poured into the mixture in small increments until the mixture is fully saturated. The mixture is stirred into a fluid like state using a small paintbrush. If the mixture is too thin it is allowed to sit for a short time to let some of the alcohol evaporate. The final thickness of the coating depends on the consistency of the mixture. Thicker coatings require a thicker mixture of copper particles and solder so that when the mixture is poured on the substrate it will not spread thin. The substrate is sanded with 200 grit sand paper until the surface is smooth and level and is followed by 600 grit sand paper to reduce the number of small scratches in the substrate.

TCMC containing 120µm particles has not been used before and the procedure for making this coating evolved to produce the best possible bonding. The mixture of copper particles to solder paste is four parts copper to three parts solder by weight. Alcohol is then added to the mixture and mixed thoroughly with a small paint brush. The surface of the substrate is sanded the same as the 75µm particle coating but after sanding a thin film of flux is applied to the surface to help the particle/solder mixture bond to the substrate. Even with the precise preparation of the surface and particles, the bonding of the final coating based on 120µm particles was poor.

The particle/solder mixture is poured onto the substrate and then the substrate is shaken to smooth out and spread the coating mixture to the approximate thickness needed. The coating mixture sits on the substrate for thirty minutes to give time for the alcohol to evaporate

before being placed on the hot plate. While the alcohol is evaporating the hot plate is set to 200°C which is 10°C hotter than the melting temperature of the plumbing solder. After all of the alcohol has evaporated the substrate is placed on the hot plate until the solder has melted. Once the solder has melted it is left on the hotplate for ten seconds and then promptly removed from the heat to avoid excessive oxidation.

2.3 Procedure For Making Extended Surface Coatings

The procedure for making coatings for flow boiling is very similar to the procedure for the coatings made for pool boiling. The copper block is sanded with 200 grit sand paper followed by 600 grit sand paper. Masking tape covers the flanged portion of the copper block so that the coating will not spread over the flanges. The coating mixture is made with the same ratio as the 1cm x 1cm pool boiling heaters. The surface area is larger in the flow boiling case and requires a larger quantity of the coating mixture. Once the coating has been applied to the copper substrate it is allowed to dry and the masking tape is removed. The particles are soldered to the substrate by heating in a temperature controlled oven for 10 minutes. The oven temperature is set to 250°C which is 60°C higher than the melting temperature of the solder.

2.4 Procedure for Cleaning TCMC

TCMC is cleaned prior to first use to remove flux residue, oxidation, and any impurities. The cleaning protocol consists of a series of baths in an ultrasonic tank and in quiescent liquid listed in Table 2.1. The alkali is an agent that clears the coating of any contaminants. The water then removes the alkali residue. The final bath is in acetone to remove oxidation.

Table 2.1 TCMC cleaning protocol

Bath	Alkali Liquid	Alkali Liquid	Water Rinse	Water	Air Dry	Acetone	Air Dry
Time (min)	12	10	2	12	1	12	1
Temperature (°C)	60	60	Room	Room		Room	
Frequency (kHz)	37	37		65		65	
Power W	1200	1200		1200		1200	

2.5 Experimental Test Procedures

All tests were ran utilizing a LabView software interface. The methodology was to apply a certain heat flux and measure the resultant temperatures. Temperature measurements were taken until the system reached steady-state and then the heat flux would be increased. Steady-state was judged by recording 100 temperatures, taking the average, and then taking 100 more temperatures and taking the average. If the difference between the two averages was less than 0.2, the system was said to be in steady-state. For flow boiling, all five thermocouple readings were required to reach steady-state by this criterion before incrementing the heat flux. Heat flux was calculated using the 4-wire method. This required measuring the voltage drop across a shunt resistor in series with the heater and measuring the voltage drop across the heater. The voltage drop across the shunt was used to calculate the current flowing through the heater. The current was then multiplied by the voltage and divided by the heater area to obtain the heat flux in the heater.

2.6 Uncertainty Analysis

The equipment and test procedures used to calculate heat flux were very similar to those of Kim in 2006 [24] and Pivovar in 2009 [25]. Thus, the heat flux uncertainty is ±6% for values ranging from 0-50W/cm^2. The equipment and test procedures for calculating flow rate and temperature are identical to that of Moreno in 2009 [3]. The uncertainty for the flow rate measurement is 1.6% and for temperature is estimated to be ±0.5°C.

CHAPTER 3

RESULTS AND DISCUSSION

Pool boiling and flow boiling tests were conducted in this study. The pool boiling tests were conducted and evaluated to find the particle size/coating thickness combination that maximized BHT. The optimized particle size/coating thickness that was found was then tested in flow boiling. Pool boiling tests were conducted with varying particle size and thickness as shown in Table 3.1.

Table 3.1 Pool boiling parameters

Particle Size (μm)	75, 120
Coating Thickness (μm)	70-1700

Table 3.2 shows the parameters that were varied for the flow boiling tests. The particle size and coating thickness were determined from the pool boiling tests. The pool boiling and flow boiling data was compared to plain copper heaters.

Table 3.2 Flow boiling parameters

Flow Rate (lpm)	0.25, 0.5, 1.0
Inlet Temperature (°C)	20, 50
Particle Size (μm)	Optimized from pool boiling study
Coating Thickness (μm)	Optimized from pool boiling study

3.1 Pool Boiling

3.1.1 References Curves

As discussed previously, the TCMC with 75µm particles were made on a 1cm x 1cm heater. Two plain copper heaters were tested and the results were compared to the Rohsenow pool boiling correlation [16] given by:

$$\left[\frac{c_{pL}\Delta T}{h_{LG}}\right] = C_{sf}\left[\frac{q''}{\mu_L h_{LG}}\left(\frac{\sigma}{g(\rho_L-\rho_G)}\right)^{1/2}\right]^n Pr_L^{(m+1)} \tag{3.1}$$

which is commonly used as a basis of comparison of pool boiling curves. For water, Rohsenow recommended m = 0 and n = 0.33. The various recommended values of surface factor, C_{sf}, are listed in Table 3.3. For this experiment the liquid-surface combination is water on polished copper which has a C_{sf} value of 0.0128.

Table 3.3 Values of surface parameter, C_{sf}, in Rohsenow correlation [16] for various combinations of metals and liquids

Liquid-Surface Combination	**C_{sf}**
n-Pentane on polished copper	0.0154
n-Pentane on polished nickel	0.0127
Water on polished copper	0.0128
Carbon tetrachloride on polished copper	0.0070
Water on lapped copper	0.0147
n-Pentane on lapped copper	0.0049
n-Pentane on emery polished copper	0.0074
Water on scored copper	0.0068
Water on ground and polished stainless steel	0.0800
Water on PTFE pitted stainless steel	0.0058
Water on chemically etched stainless steel	0.0133
Water on mechanically polsihed stainless steel	0.0130

The resulting pool boiling curves along with the Rohsenow correlation are shown in Figure 3.1. The tests show that the construction techniques and the fabrication of the heaters

were completed properly and consistently. The pool boiling curves obtained from these heaters will serve as reference curves.

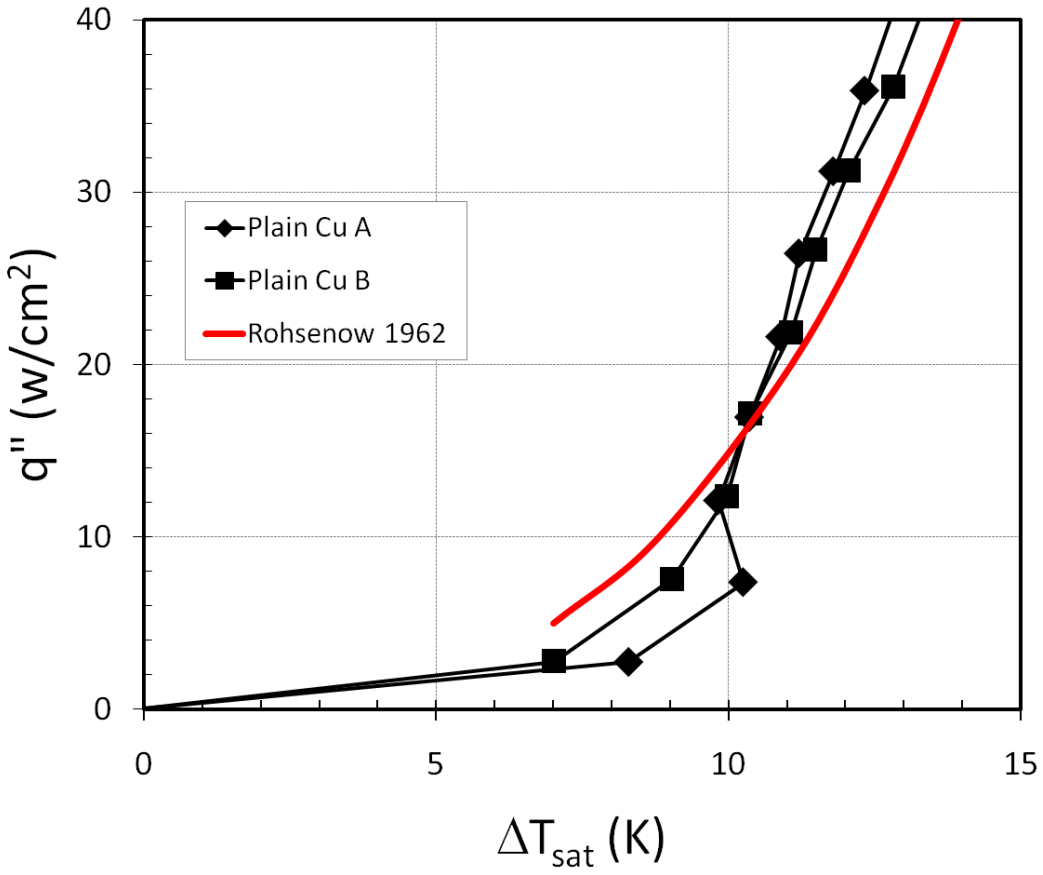

Figure 3.1 Comparison of plain copper heaters performance to Rohsenow correlation

3.1.2 Pool Boiling-75µm Particles

Particle size of 75µm has been previously used by the Micro-Scale Heat Transfer Lab at The University of Texas at Arlington at a coating thickness of ~150µm to improve both the BHT and CHF of the heater. It is expected that BHT could increase with increasing thickness up to the point where the coating introduces significant thermal resistance. You et al. [13] showed this trend with a diamond particle and epoxy coating. As the coating paint thickness increased

the surface temperature increased due to the thermal conduction resistance of the coating. Throughout this study the coating whose thickness yields best performance in BHT will be referred to as the coating with the optimal thickness. Heaters were made with various thicknesses of coatings and tested in pool boiling as prescribed in chapter 2. The results and reference curve for plain heater are shown in Figure 3.2.

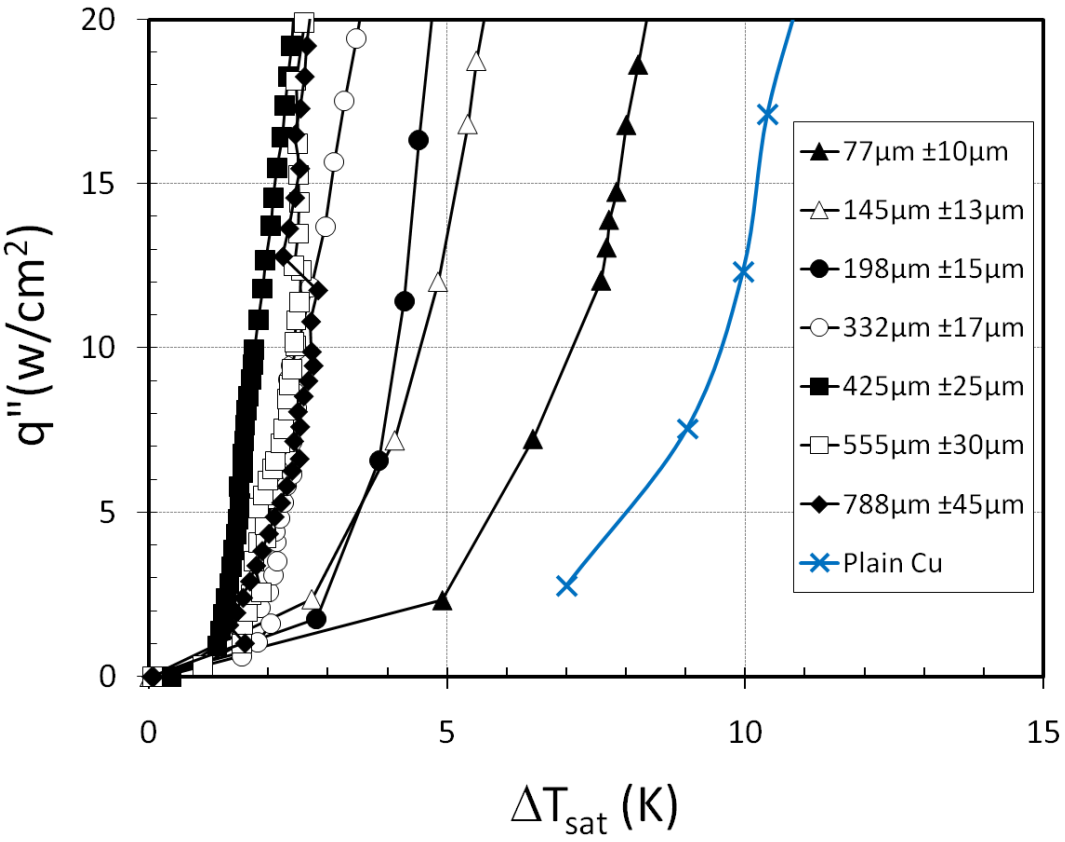

Figure 3.2 Pool boiling results for 75µm particle coatings at various thicknesses

The boiling heat transfer curves in Figure 3.2 show increase in BHT as thickness increases, except for the two thickest coatings. The greatest increase in BHT occurs for the 425µm±25µm thick coating. Figure 3.3 clearly illustrates this through heat transfer coefficient

versus coating thickness. The heat transfer coefficients (h) were calculated at a heat flux of ~12W/cm^2 for all of the thicknesses.

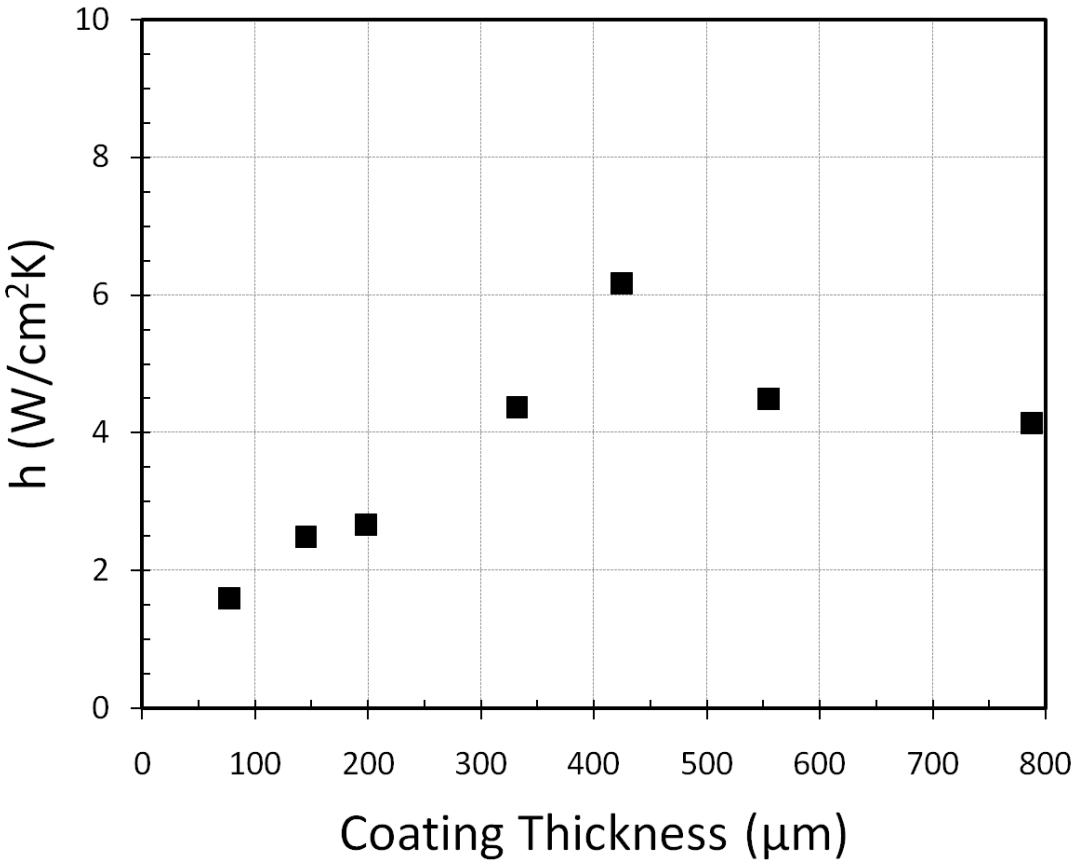

Figure 3.3 Effect of coating thickness on heat transfer coefficient for 75µm particles

3.1.3 Pool Boiling-120µm Particles

The 120µm particles have not been used in the research of TCMC and a mixture ratio to successfully bond this coating had to be found. This was done by starting with the ratios for the 75µm particles and adjusting the ratio from there. The ratio of copper particles to solder of 2 to 1 did not provide proper bonding strength. During the ultrasonic treatment of the cleaning protocol most of the particles detached from the substrate. The new ratio was 4 parts copper to

3 parts solder. When this coating was cleaned in the ultrasonic bath little to no particles were released from the substrate.

Previous studies have shown that coatings with larger particles produced more nucleation sites and resulted in pores with better vapor entrapment capabilities, optimizing heat transfer enhancement. Sarwar et al. [1] increased particle sizes ranging from 1-10µm and this suggested that if the particle sizes were increased from 75µm to 120µm the BHT could be enhanced. Figure 3.4 shows the results of the pool boiling tests with the 120µm particles. The 120µm particles show an optimal thickness, for BHT, much like the 75µm particle coatings, which is 783µm±28µm.

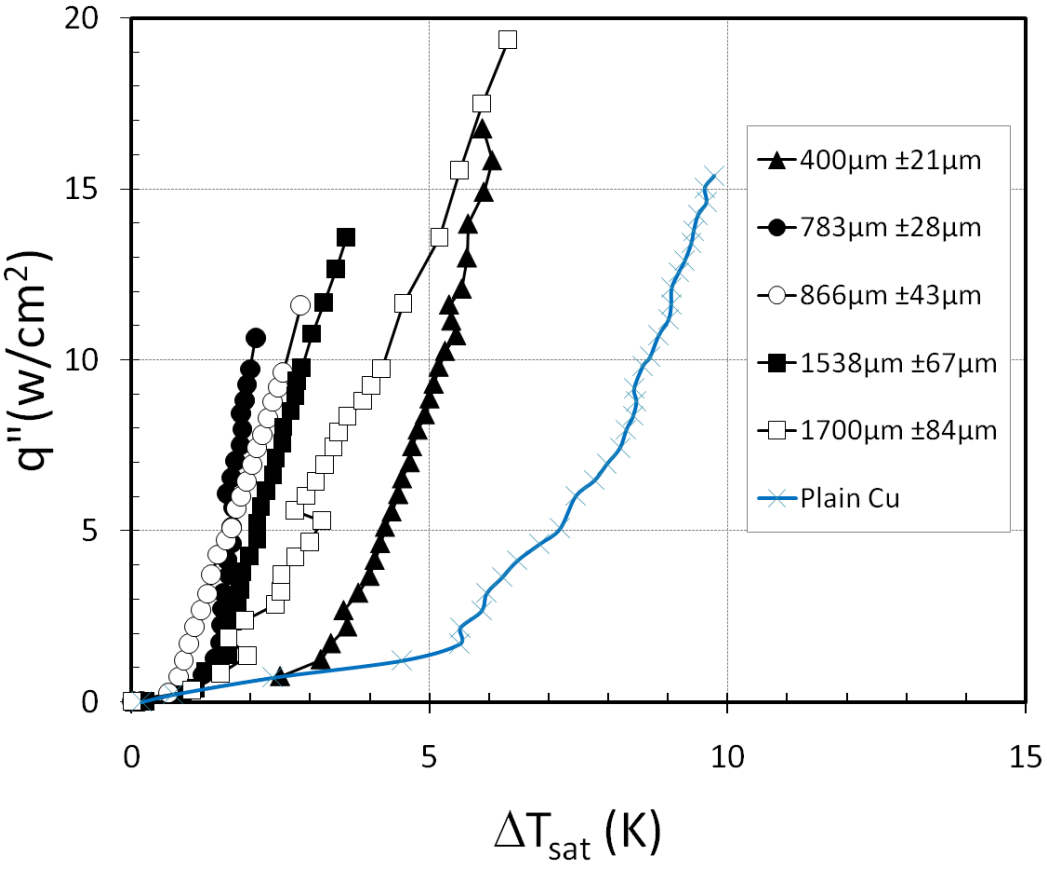

Figure 3.4 Pool boiling results for 120µm particle coatings at various thicknesses

As the thickness of the coating increases beyond 783µm±28µm, the BHT decreases as seen by a shift to the right in the boiling curve, most probably due to thermal resistance increase as seen by You et al. [13] with the diamond particle and epoxy coating. Figure 3.5 shows the heat transfer coefficient versus the coating thickness for the 120µm particles. The h values were calculated at a heat flux of ~10W/cm^2 for all of the thicknesses. This shows that the greatest h value occurs at 783µm±28µm.

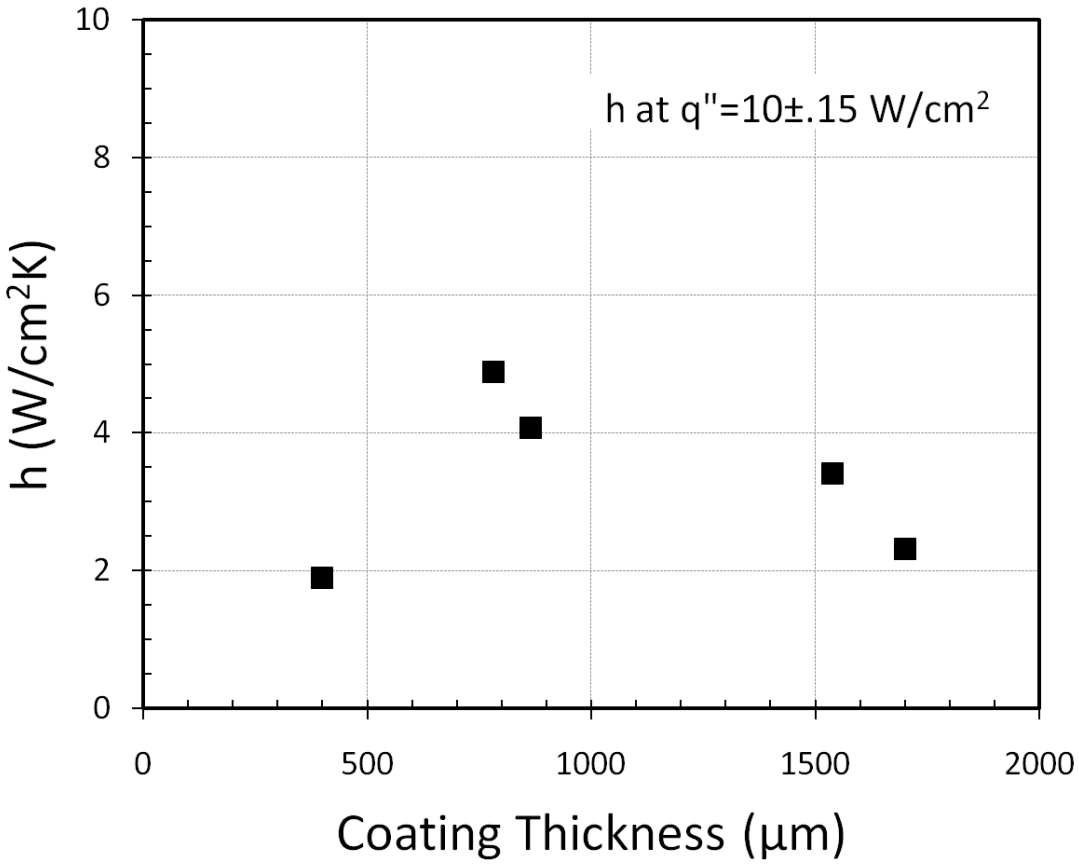

Figure 3.5 Effect of coating thickness on heat transfer coefficient for 120µm particles

3.1.4 Comparison of Optimal 75µm and 120µm Particles

The pool boiling curves for the two optimal thicknesses are compared (Figure 3.6) along with the data labeled as Kwark Best TCMC [26]. Kwark Best TCMC is a coating that is roughly 150-170µm thick and was previously produced in the Micro-Scale Heat Transfer Lab at The University of Texas at Arlington. This is shown to compare to a coating of similar thickness (145µm±13µm) produced in this study. The difference in the two BHT curves ranges from less than 1°C at lower heat fluxes to about 2°C at higher heat fluxes. The differences are believed to be a result of differences in technique or skill in making the heaters and coatings. However, within the technique of this study, the coated heaters are repeatable as Figure 3.7 illustrates, which compares pool boiling curves obtained over two coated heaters utilizing the same particle size and similar coating thickness, and therefore the optimization should be valid for this study. Figure 3.6 also shows that there was no significant enhancement difference between the optimized coatings for the 75µm and the 120µm particles. Therefore the 75µm particle only was selected for the flow boiling study and the bonding problems with the 120µm particles were thereby avoided.

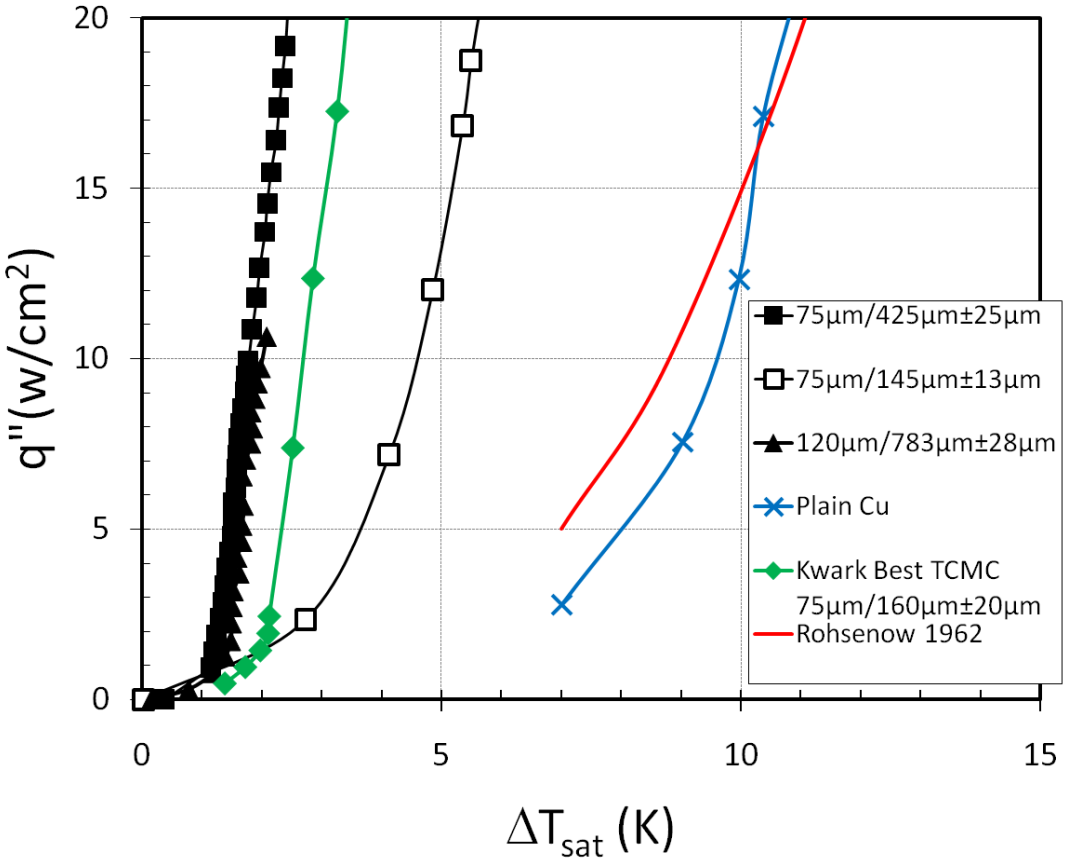

Figure 3.6 Comparison of optimized coatings

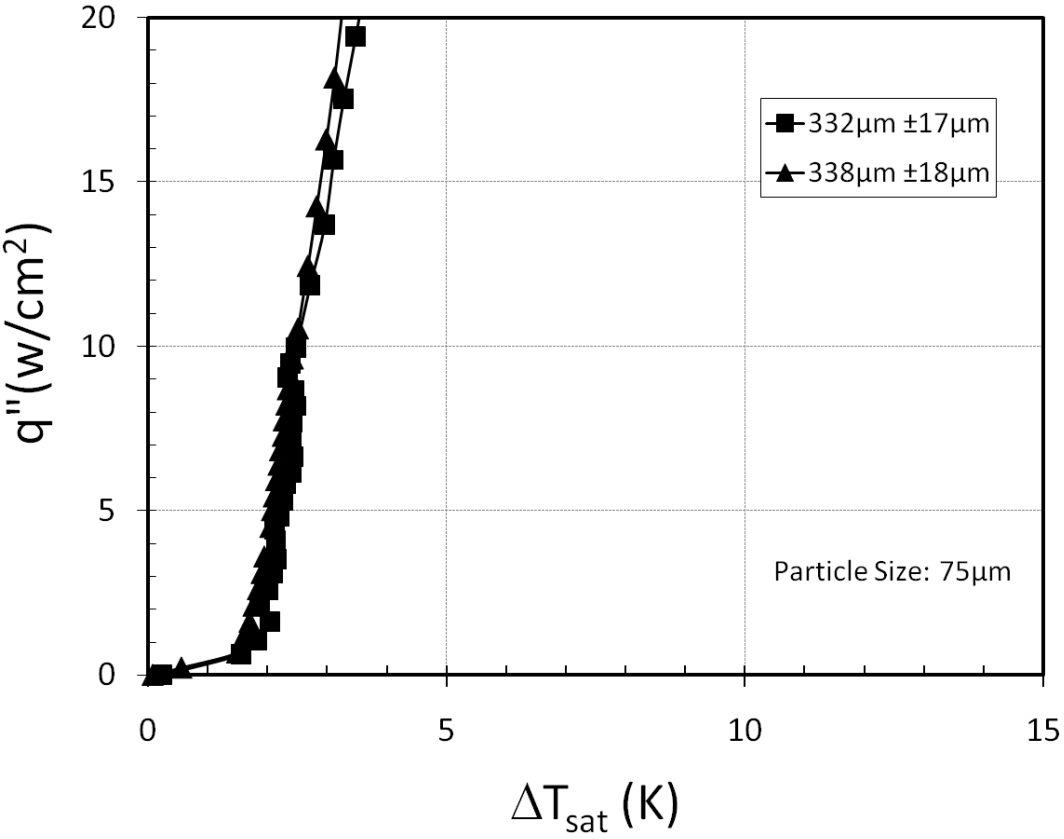

Figure 3.7 Repeatability of coating generation technique

3.2 Flow Boiling

Flow boiling tests were performed as described in Chapter 2. Tap water was used for this experiment to resemble conditions seen by a tankless hot water heater. The setup of the test section is shown in Figure 2.5 and originally silicone was used to seal the lexan components together to prevent leaks. During the initial runs of tests higher temperatures in the coated heater relative to the plain heater were noticed. In investigating the cause it was found that silicone had wicked into the edge of the coating. Figure 3.8 illustrates the pattern of contamination suggested from visual inspection. Therefore the effect of silicone contamination was studied to prove that it was the cause of the higher temperatures.

3.2.1 Effect of Silicone Contamination

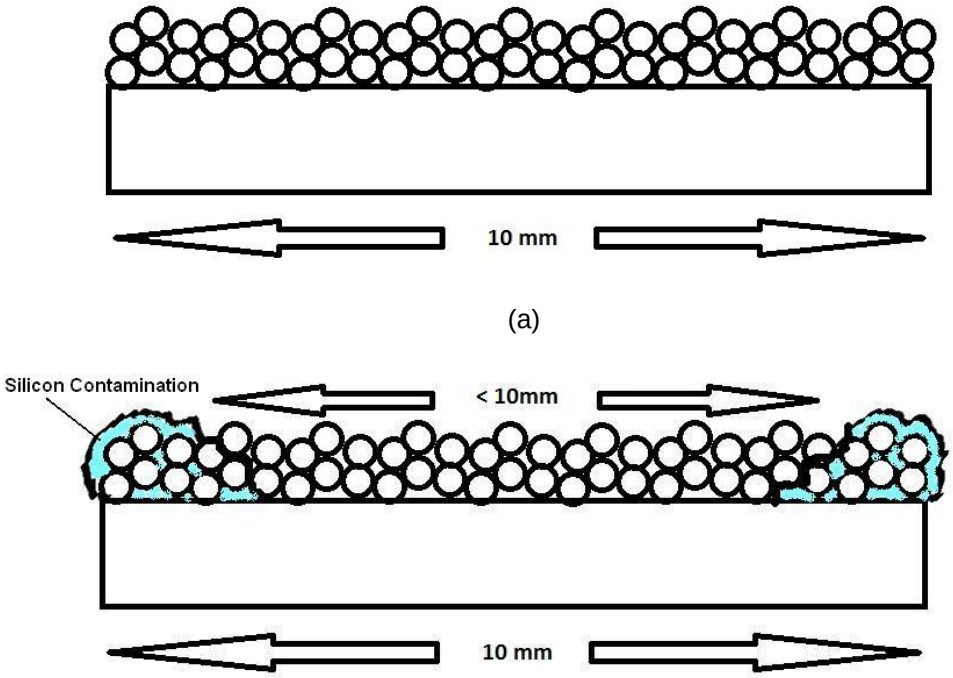

Figure 3.8 Cross section illustration of (a) clean TCMC and (b) perimeter contamination on TCMC

It is difficult to quantify exactly how much of the coating was contaminated since some of the silicone could have penetrated deeper than what is visible from the outside. To determine the effect of this contamination on BHT, a 1cm x 1cm heater was coated and tested in pool boiling, and then was purposefully contaminated and tested in pool boiling again. Figure 3.9 shows microscope images of the clean and contaminated samples.

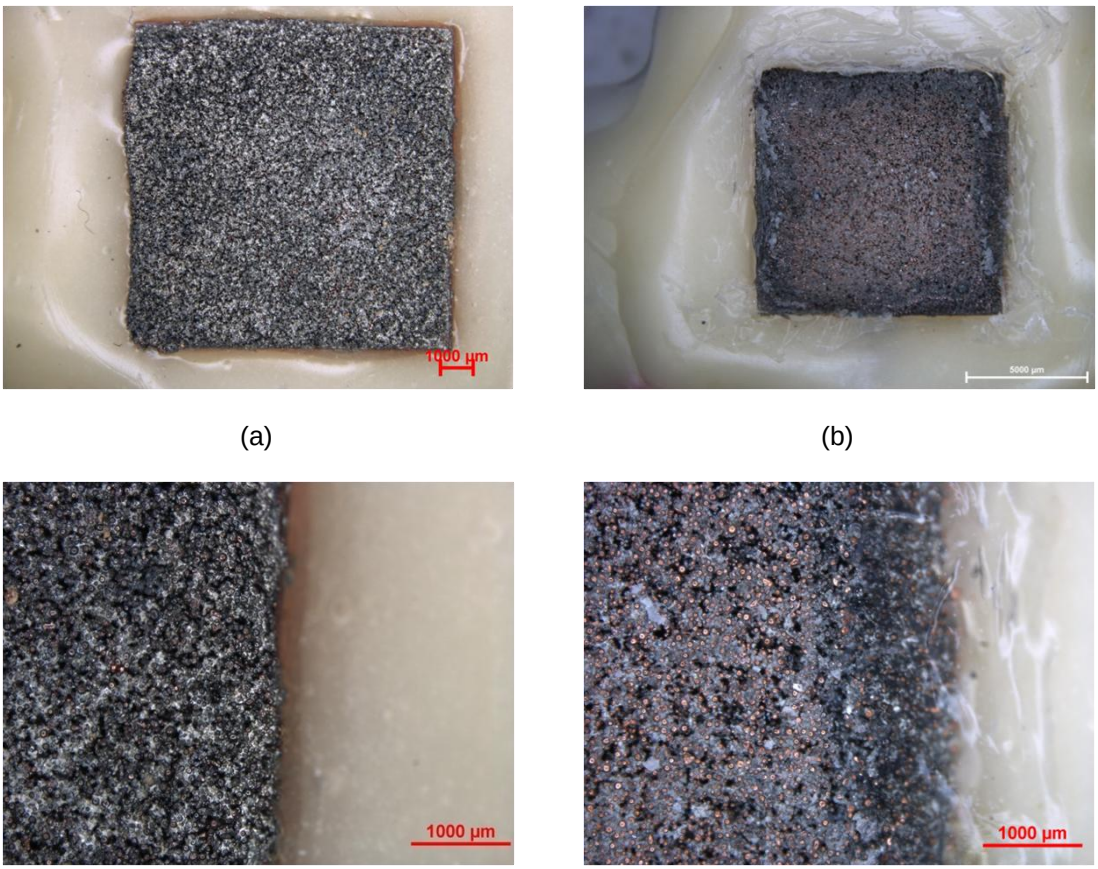

Figure 3.9 Microscope images of (a) full view clean coating, (b) full view silicone contaminated coating, (c) close up of edge of clean coating, and (d) close up of edge of silicone contaminated coating

The test was performed at both gassy-subcooled conditions and in saturated conditions. Gassy subcooling is when a liquid is at a temperature lower than the saturation temperature at a given pressure, and noncondensable gases, such as ambient gases, are dissolved into the liquid. The resulting gassy-subcooled pool boiling curves were recorded in Figure 3.10. The temperature difference in the remaining curves that show subcooled data will be labeled as T_{sur}-100°C, instead of ΔT_{sat}, since 100°C, the saturation temperature of water at 1atm, is a reference temperature and not the actual bulk temperature of the water. These tests were conducted at 50°C subcooled which means that the bulk temperature of the water was

maintained at 50°C below the saturation temperature, 100°C, for the system pressure of the test (1 atm). There appears to be a large increase of up to 10°C in the surface temperature in the natural convection region for the contaminated coating (open rectangles). When the curve transitions to fully developed boiling (FDB) the shift becomes less prominent. The shift in the natural convection region is accredited to the insulating properties of the silicone. It was estimated that the uninsulated area of the contaminated coating was less than that of the clean coating by ~25% which in turn increased the heat flux by ~28% for a given power input. The boiling curve for the contaminated coating (open rectangles) appeared shifted to the right because it was plotted using the wrong heat flux values, that is, the heat fluxes based on assuming a clean coating. When the heat fluxes were adjusted for the reduced area due to the contamination (open diamonds, Figure 3.11), the two curves matched (Figure 3.11). For example if the heat flux was 10W/cm^2 and the original area was 1cm^2 then the reduced area heat flux was ~13.8W/cm^2. The testing apparatus was sealed with Teflon for the remainder of the study to avoid the contamination.

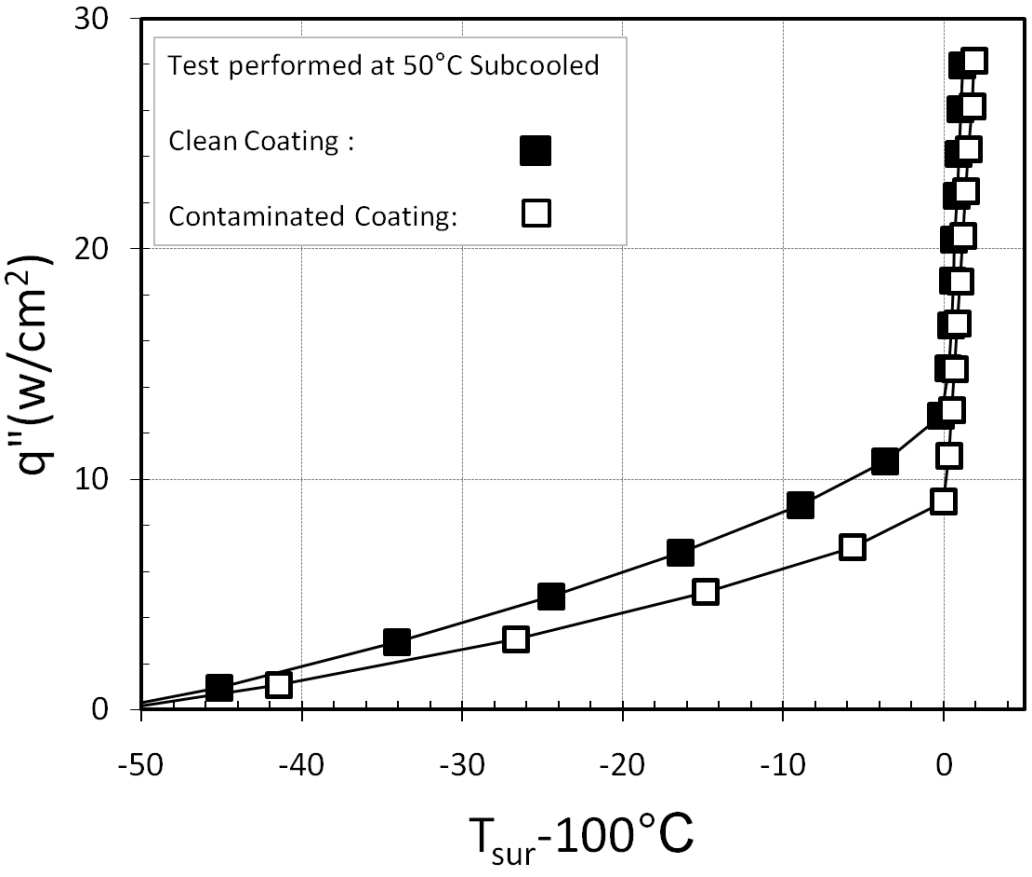

Figure 3.10 Effect of silicone contamination on coated surface in subcooled test

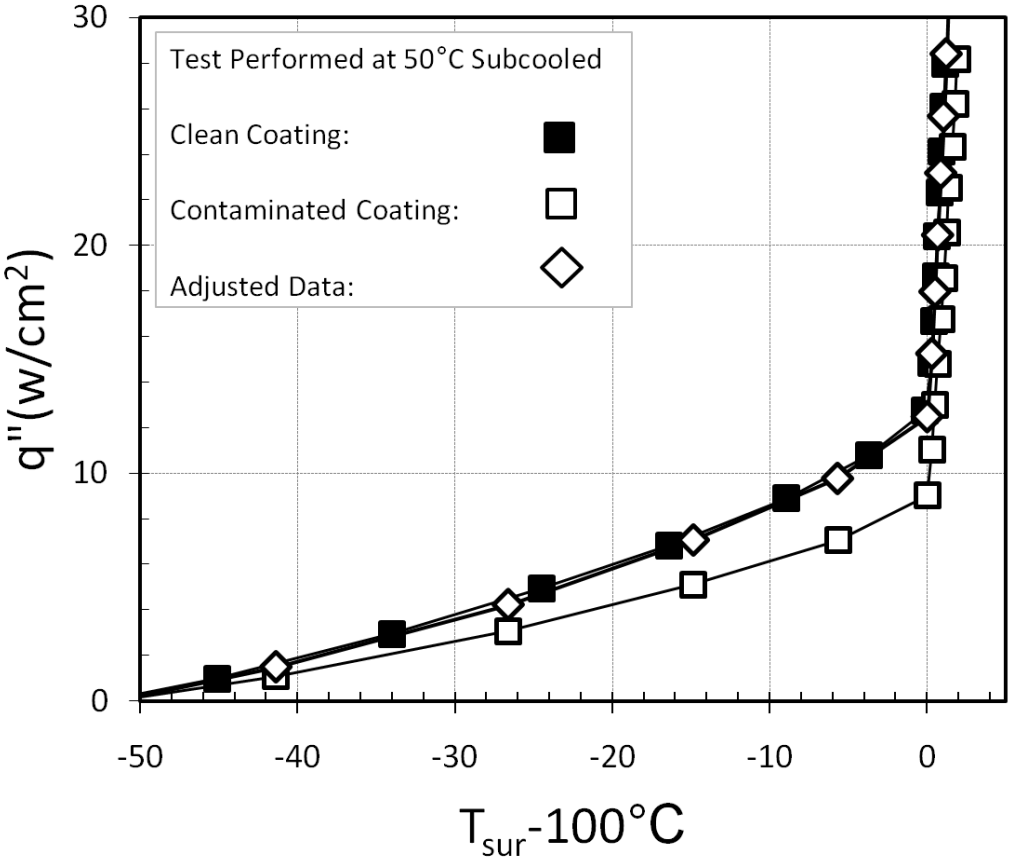

Figure 3.11 Boiling curve adjusted for correct area

3.2.2 Flow Boiling Parameters

The flow boiling parameters were discussed previously, and are redisplayed in Table 3.4 along with the resulting mean velocities and average Reynolds numbers. The average Reynolds numbers were calculated based on fluid properties at ranging temperatures. Laminar flow is defined as a Reynolds number below 2300 for internal flow. The Reynolds number for .25lpm indicates laminar flow, for 1lpm indicates turbulent flow, and for .5lpm indicates transition to turbulent. The mean velocity was calculated using the flow rate and the channel cross-sectional area given in Figure 3.12.

Table 3.4 Flow boiling parameters and resulting flow values

Inlet Temperature (°C)	20		50
Gassy-subcool Level (°C)	80		50
Flow Rate (lpm)	0.25	0.50	1.00
Average Velocity (m/s)	0.08	0.16	0.32
Average Re	1182	2364	4728

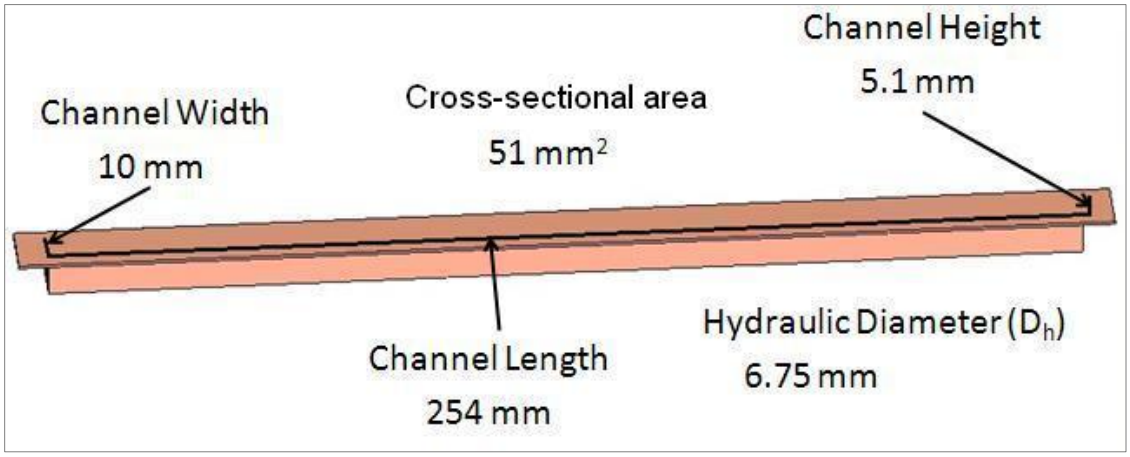

Figure 3.12 Copper block with dimensions

3.2.3 Subcooling at 80°C

The boiling heat transfer curve is produced in a similar way to the pool boiling curve. The heat flux is set to a certain value and the control program waits for the 5 thermocouples to reach steady-state and records all of the temperatures. This is repeated until the desired maximum heat flux is reached or the system cannot provide any additional power. Due to the larger area of the heater compared to the heaters used in pool boiling, to generate a given relatively low heat flux, significantly higher powers were required. For example, approximately 500W were required to reach a heat flux of about 20W/cm^2, but only 20W for the 1x1cm^2 heater in pool boiling.

Figure 3.13 shows the curves for the test case, 80°C subcooled, (inlet temperature of 20°C), and volume flow rate of 0.25lpm, corresponding to locations of thermocouples 1 and 3. Both the plain and coated heaters display similar temperatures for same heat fluxes below ~6W/cm^2. This occurs since both of the heaters are in the single-phase forced convection region where the coating has no prominent effect. For the plain copper surface (closed symbols), at heat fluxes of 12W/cm^2 and 14W/cm^2, corresponding to T3 and T1, respectively, the surface temperatures abruptly decrease (seen as a sudden jump or step-up in the curve).

In an effort to better understand these abrupt temperature changes, along with making visual inspections, photographs were taken during the tests of both the plain and coated heaters. The photographs are shown in Figure 3.14 and Figure 3.15, for plain and coated heaters respectively. These photographs were taken at some time or times during the transient processes between programmed heat flux increments. For example, Figure 3.14(b) is a photograph taken after the heat flux had been incremented by 2W/cm^2 from a steady-state at 10W/cm^2, but before the new steady-state had been reached. Therefore the photograph is labeled as being between 10W/cm^2 and 12W/cm^2 in the caption. In one case, Figure 3.14(d), multiple photographs were taken over a period of time because the system took significant time to reach steady state.

Photographs taken for heat fluxes of 12W/cm^2 (Figure 3.14(b)) and 14W/cm^2 (Figure 3.14(c)) reveal that a significant number of bubbles had appeared on the plain heater over this range of heat fluxes. Even though the surface temperatures corresponding to these heat fluxes are well below saturation temperature (100°C), the sudden jump in the curves could be due to phase change, or, even though no departing bubbles were visually detected, due to partial boiling. At a high level of subcooling it is possible that in partial boiling the departing bubbles very quickly condensed allowing too short a time for visual detection. Phase change is possible at a surface temperature significantly below saturation temperature due to the high degree of gassy subcooling. Subcooling allows a large amount of non-condensable gases to dissolve in

the water, and the flow mixes the liquid and non-condensable gas together. As the surface temperature increases, bubbles readily form in the microcavities that are present on the heated surface. The pressure inside the bubble is then the sum of the partial pressures of the vapor and gas, so that the individual pressures are less than 1atm. With a vapor pressure of less than 1atm inside the bubble, phase change can occur at less than 100°C.

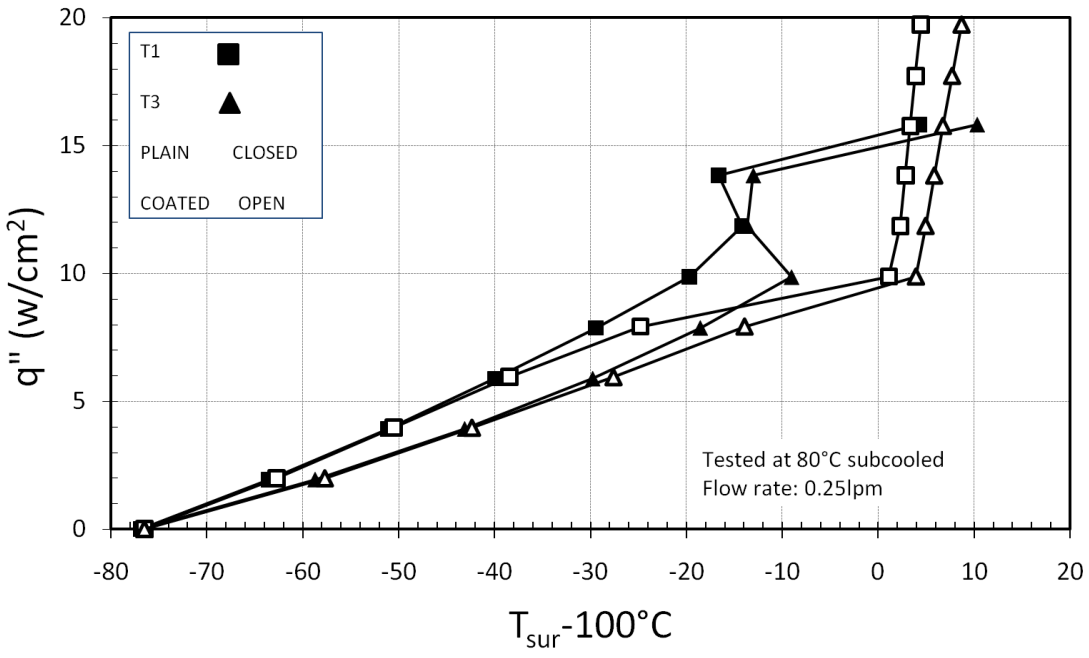

Figure 3.13 Flow boiling curve for plain and coated at 0.25lpm and 80°C subcooled

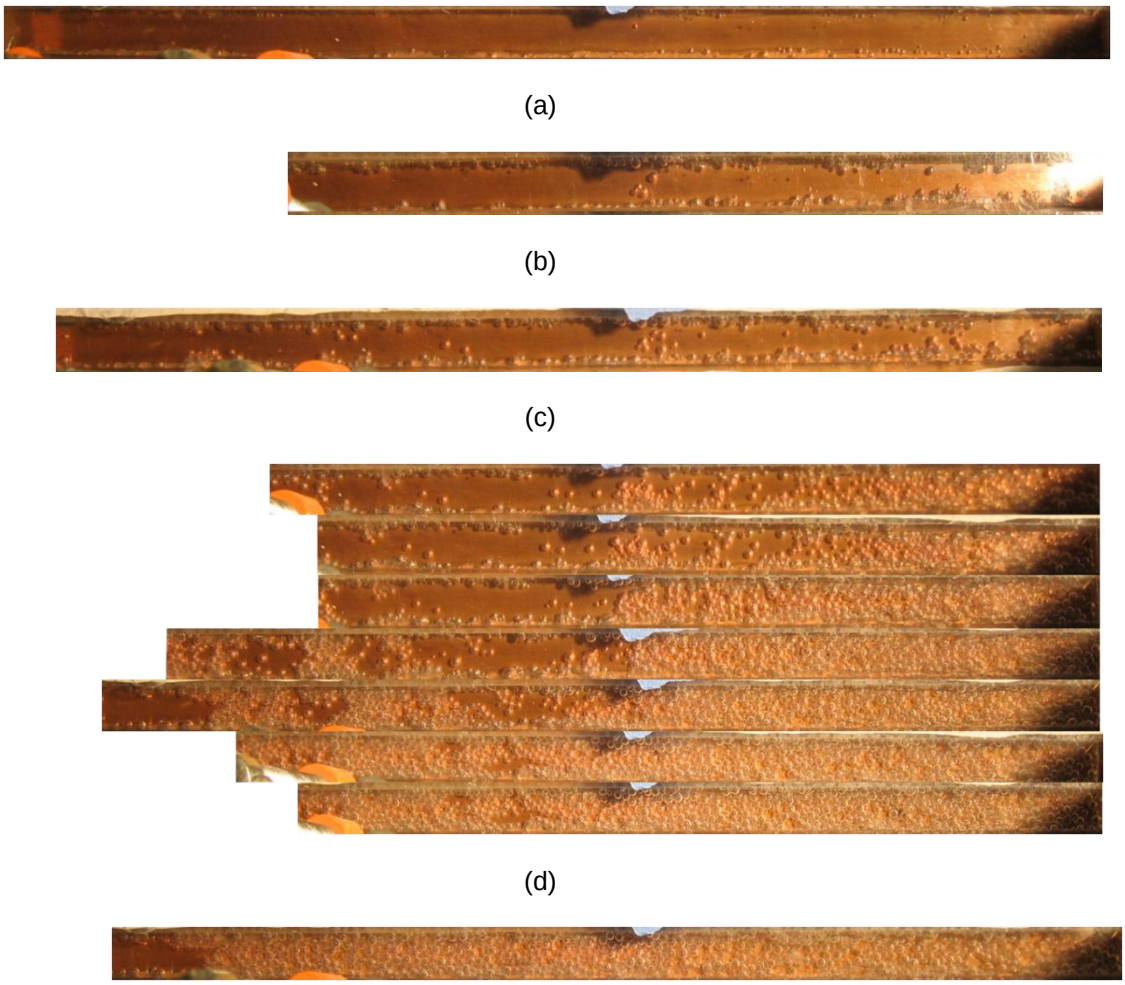

(a)

(b)

(c)

(d)

(e)

Figure 3.14 Bubbles on plain surface between (a) 6W/cm^2 - 8W/cm^2, (b) 10W/cm^2 - 12W/cm^2, (c) 12W/cm^2 - 14W/cm^2, (d) 14W/cm^2 - 16W/cm^2, and (e) 16W/cm^2 - 18W/cm^2

In Figure 3.13, for the plain heater, the beginning of partial boiling is detected at the downstream location when the heat flux is 12W/cm^2 and for the upstream location when the heat flux is at the higher value, 14W/cm^2. This is due to the accumulated heat input at the downstream end of the heater. For the next heat flux increment from 14 to 16W/cm^2, the number of bubbles that are stationary on the plain heater continuously increases while the system reaches the new steady-state at 16W/cm^2 (Figure 3.14 (d)). This increasing number of

bubbles acts as a gas and vapor blanket that covers and insulates the whole heated surface. This could explain the dramatic increase in surface temperature observed in Figure 3.13 for the plain heater, when the heat flux is incremented from 14W/cm^2 to 16W/cm^2. The photograph in Figure 3.14(e) is included to display the blanket of bubbles soon after a steady-state had been reached for 16W/cm^2, which corresponds to the beginning of the process to reach steady-state at 18W/cm^2. This particular test over the plain heater was terminated before reaching this steady-state. However, Figure 3.16, which shows results for heat fluxes above 18 W/cm^2 at the same subcooling level and at 0.25lpm flow rate, shows that the plain heater transitions into FDB.

In Figure 3.13, for the coated heater (open symbols), other than the onset of FDB at 10W/cm^2, there is no separate jump in the curves (due to phase change). This is possible because the coating increases the number of microcavities on the surface. At heat fluxes lower than for the plain heater, the coated heater more readily produces bubbles within the microcavities. At the lower heat fluxes, the great majority of these bubbles are stationary, blanketing the surface at heat fluxes lower than for the plain heater. For example, compare Figure 3.15(c) to Figure 3.14(a), each showing an instance of the heated surface, coated and plain respectively, between 6W/cm^2 and 8W/cm^2. The gas-vapor blanket has the effect of raising the surface temperature more than the phase change can reduce it. This is probably why in Figure 3.13, starting at a heat flux of about 8W/cm^2, the temperatures of the coated heater are greater than those of the plain heater. The FDB regime occurs after 10W/cm^2. This is seen by the very high slope reflecting the very little temperature change with increasing heat flux. Moving bubbles due to FDB cannot be told apart from stationary in Figure 3.15(e), a photograph taken between 12W/cm^2 and 14 W/cm^2, which are heat fluxes falling within the FDB regime, but visual inspection confirmed that significantly numerous bubbles were departing and flowing down the channel. Further examination of the bubble phenomenon can be seen in Appendix A.

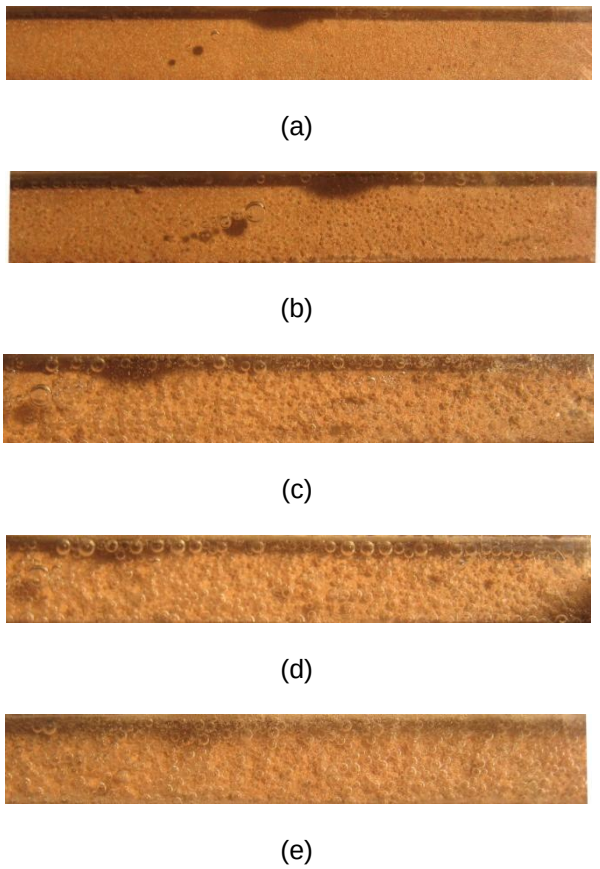

Figure 3.15 Bubbles on coated surface between (a) 2W/cm^2 - 4W/cm^2, (b) 4W/cm^2 - 6W/cm^2, (c) 6W/cm^2 - 8W/cm^2, (d) 8W/cm^2 - 10W/cm^2, and (e) 12W/cm^2 - 14W/cm^2

Figure 3.16 displays the results of all the tests at ~80°C subcooling for both plain copper and coated heaters at three flow rates. The temperatures in the figure are obtained by averaging the temperatures of all three thermocouple locations. Like in Figure 3.13 the temperatures at low heat fluxes (<5W/cm^2) for plain and coated heaters are similar because the heat transfer is all in single-phase and therefore the vapor trapping abilities of the coating have no opportunity to exercise any influence. At about 10W/cm^2 there are abrupt slope shifts which signify the onset of partial boiling. Beyond 10W/cm^2 stationary gas-vapor bubbles blanketed the surface of the coated heater for all flow rates but not the plain heater, and again this could explain why the temperatures of the coated heater are higher than those of the plain heater.

Starting at a heat flux of about 15W/cm^2 however, this trend starts to reverse for the lower flow rates (0.25lpm, 0.5lpm). Over the coated heaters, partial boiling transitions into fully developed boiling and the curves cross over those of the plain heaters at ~16W/cm^2 and ~24W/cm^2 for 0.25lpm and 0.50lpm respectively, after which the coated heaters are lower in temperature than the plain heaters. Eventually, therefore, the coating provides the expected enhancement in the FDB region (higher heat flux at a given surface temperature or lower surface temperature for a given heat flux). In terms of temperature, for 0.25lpm and 0.5lpm at 25W/cm^2, the coated heater is operating ~7°C cooler than the plain, and this temperature difference is maintained for a range of lower heat fluxes for the 0.25lpm case. Enhancement is not seen at the flow rate of 1.00lpm because the available power was not sufficient to provide the additional heat input necessary to initiate fully developed boiling at the higher flow velocity. Otherwise, also for 1.00lpm, the curve for the coated heater would not remain to the right of that of the plain, indicating higher temperatures, but would cross over and reach FDB at a lower temperature than for the plain heater. Therefore, given a sufficiently high heat flux, the TCMC heater enhances BHT. However, the highest volume flow rate is also a strong source of heat transfer enhancement. The higher flow velocity and the turbulence at 1lpm act to deliver and replenish the noncondensables more effectively to the microcavities in the surfaces (plain or coated). This interaction with the noncondensables produces more intense partially developed boiling relative to the lower flow rates. This is revealed in the slight upward divergence or separation in the curves for 1lpm from the curves for the other flow rates. However, the partially developed boiling enhancement on the coated heater at 1lpm (open triangles) is not as strong above 20 W/cm^2 as on the plain heater, probably because vapor-gas bubbles blanket the coated surface more thoroughly. In any case, for both plain and coated heaters, a clear trend of enhancement of partially developed boiling heat transfer with increasing volume flow rate is seen.

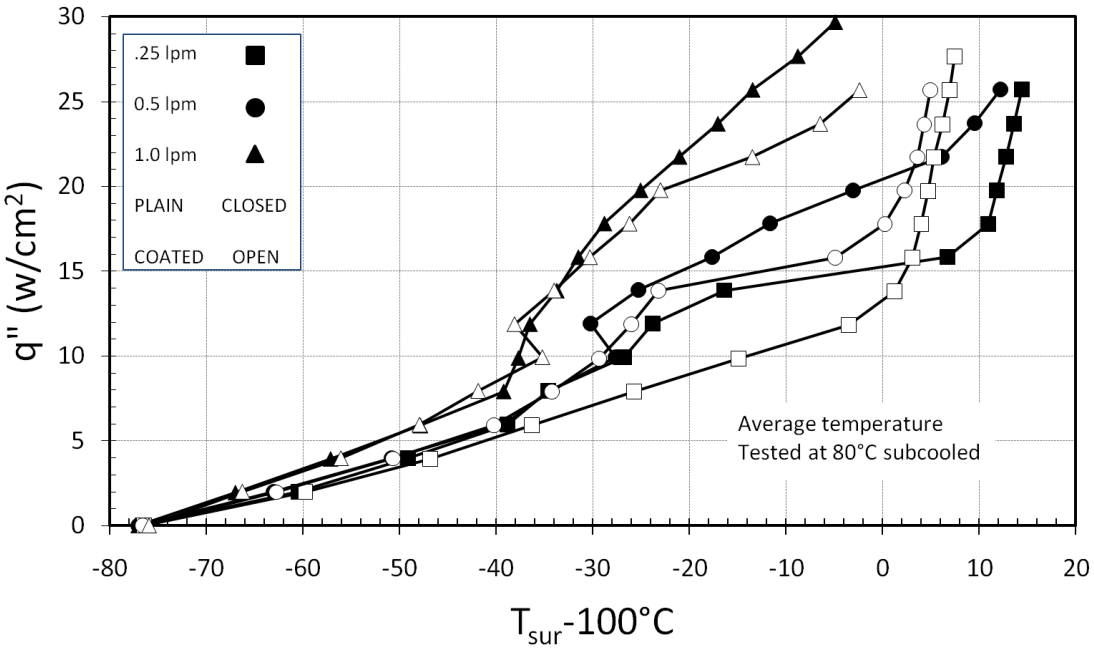

Figure 3.16 Effect of flow rate at 80°C subcooling for coated and plain heaters

Figure 3.17 is a plot of the average heat transfer coefficient in terms of heat flux, and flow rate for the coated heater. The average heat transfer coefficient is obtained by averaging the heat transfer coefficients at all three thermocouple locations. All three curves show a tendency for increasing heat transfer coefficient with increasing heat flux, except for sudden shifts and drops which would have to be connected with the onset of partial boiling (increases in slope) and the subsequent accumulation of stationary gas-vapor bubbles (decreases in slope). These are followed by steady climbs in heat transfer coefficient for 0.25lpm and 0.50lpm which occur upon the arrival of FDB, at around 14W/cm^2, since nucleating bubbles are able to depart in spite of the gas-vapor blanket, and thereby latent heat transfer dominates. No such steady climb is seen in the curve for 1.00lpm reflecting that FDB was not reached, as was also seen in Figure 3.16. Figure 3.17 also shows that the heat transfer coefficient increases with increasing flow rate, and significantly so in the partially developed boiling region, reflecting that forced

convection acts to feed noncondensables to the surface and thereby promote partially developed boiling, as was already observed in Figure 3.16. Flow rate has less effect on the FDB region which is reached for both 0.25lpm and 0.50lpm, where phase change is the dominant mode of heat transfer.

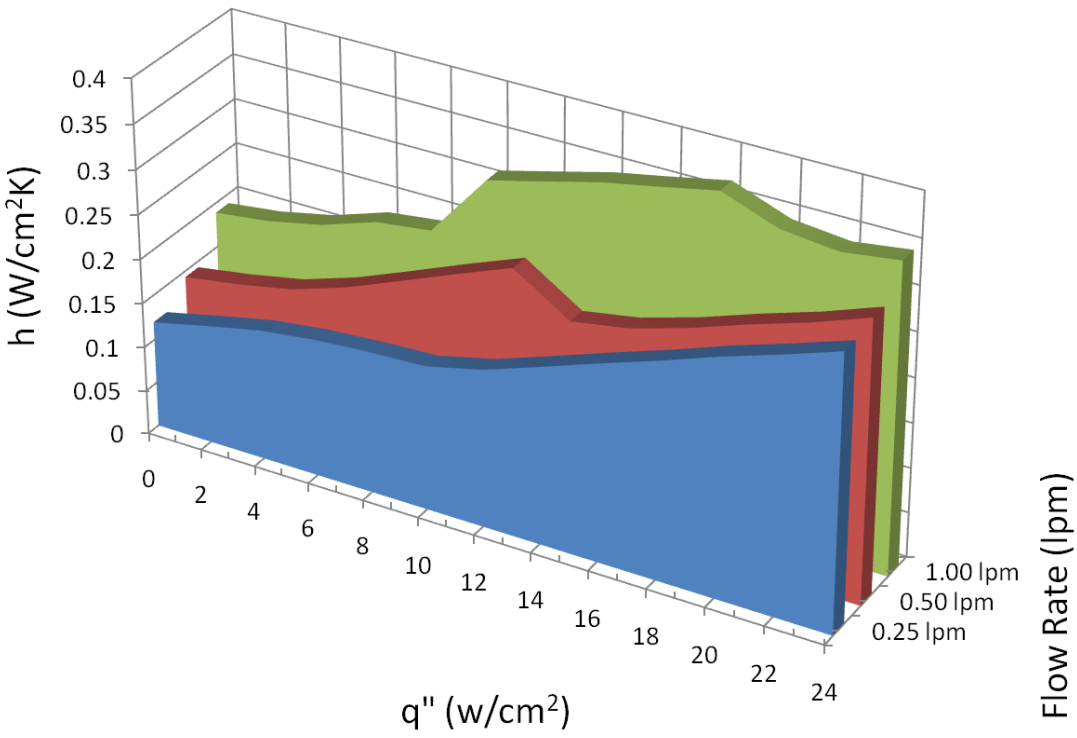

Figure 3.17 3-D Plot of heat transfer coefficient, heat flux, and flow rate for coated heater at 80°C subcooled

3.2.4 Subcooling at 50°C

Flow boiling tests were performed at 50°C bulk temperature (equivalent to 50°C subcooling), to insure that FDB was reached at all flow rates (Figure 3.18). Like Figure 3.16,

Figure 3.18 shows that at the low heat fluxes, ~4W/cm^2 and below, the coated and plain heaters have similar temperatures since the heaters are in the single-phase forced convection. It is also seen that at higher flow rates (0.5lpm, circles and 1.0lpm, triangles) a slope shift appears near 4W/cm^2, much like the 80°C subcooled case, indicating the start of partially developed boiling. Also like in the higher subcooled case (Figure 3.16), there is a tendency for the temperature increase to become larger with heat flux increment towards the end of the partially developed boiling region, for both coated and plain heaters. This is due to the accumulation of gas-vapor bubbles which blanket the heaters. But unlike Figure 3.16, as they approach FDB, the coated heater shows less of a tendency to overheat relative to the plain heater, and then to cross over into cooler temperatures relative to the plain heater. Following the temperature increases, therefore, the coated heater goes into FDB for all three flow rates, while the plain heater increases in temperature further and then starts to transition into FDB. The coated heater therefore enhances BHT relative to the plain heater, and the trend of enhancement in Figure 3.18 suggests more relative enhancement could have been possible if more power could have been supplied. As expressed in section 3.2.3, the enhancement can be taken as increased heat flux for a given surface temperature, or lower surface temperature for a given heat flux. At ~25 W/cm^2, the coated heaters are operating ~10°C cooler than the plain heaters for all three flow rates. The effect of flow rate on heat transfer is less prominent than seen in Figure 3.16, since the subcooling is less. With less subcooling there are less noncondensables dissolved in the liquid, therefore there are less noncondensables available to replenish the microcavities through the mixing and flowing of the liquid.

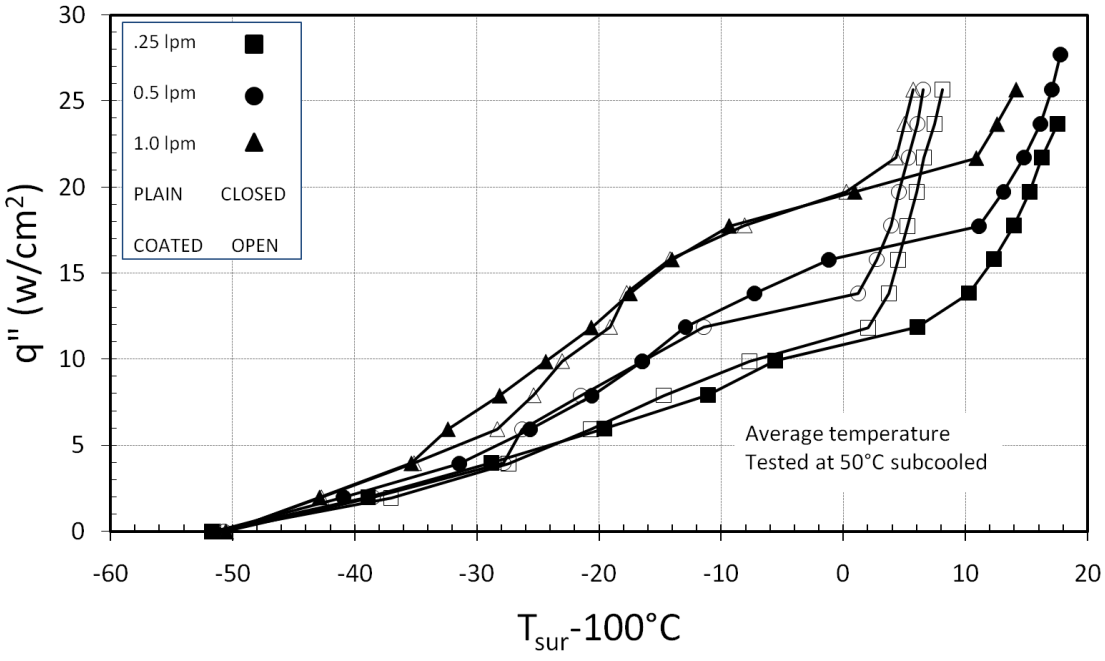

Figure 3.18 Effect of flow rate at 50°C subcooling for coated and plain heaters

Figure 3.19 shows heat transfer coefficient as a function of heat flux and flow rate for 50°C subcooling. The trends seen for the previous case are also seen with 50°C subcooling. All three curves show a tendency for increasing heat transfer coefficient with increasing heat flux, except for sudden shifts and drops which would have to be connected with the onset of partial boiling (increases in slope) and the subsequent accumulation of stationary gas-vapor bubbles (decreases in slope). As the heat flux begins to reach higher levels, the heater reaches FDB and the heat transfer begins to steadily increase due to latent heat transfer. Figure 3.19 illustrates that in 50°C subcooling the effect of volume flow rate on the partially developed boiling regime remains prominent, however, graphical confirmation of the reduced sensitivity to flow rate in the FDB regime is found. The height differences between the three curves in the FDB region are less compared to the height differences between them in most of the remaining parts of the plot.

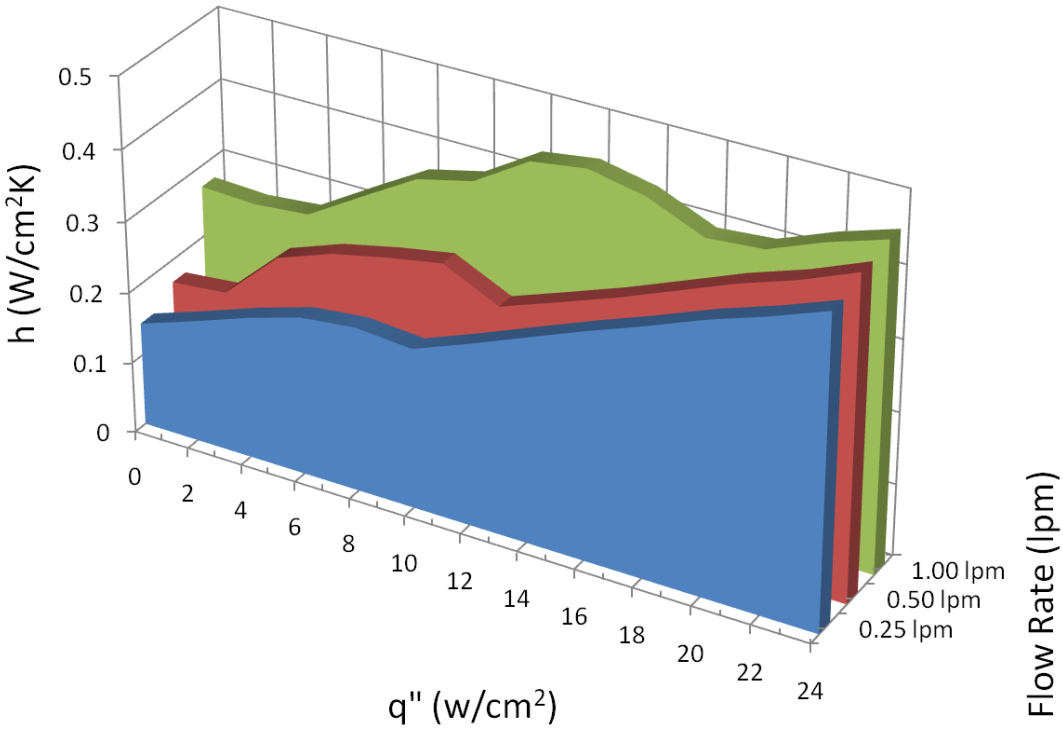

Figure 3.19 3-D Plot of heat transfer coefficient, heat flux, and flow rate for coated heater at 50°C subcooled

3.2.5 Comparison of Flow Boiling to Pool Boiling

A comparison of a 50°C subcooling case for flow boiling (average wall temperature) and 50°C subcooling test in pool boiling over a 1cmx1cm coated heater (75µm particles, 425µm±25µm thick) shows significant differences (Figure 3.20). For heat fluxes below 10W/cm^2, the flow boiling curve shows enhancement as the temperatures are lower for the same heat fluxes. This is expected since the introduction of forced convection enhances the heat transfer. In the FDB region, the pool boiling curve shows better performance than flow boiling. A factor in this difference is that in order to induce the flow, the pressure in the flow boiling test section

could be slightly higher than the pressure of the pool boiling test, which is 1 atm. The higher pressure leads to higher saturation temperature, greater than 100°C.

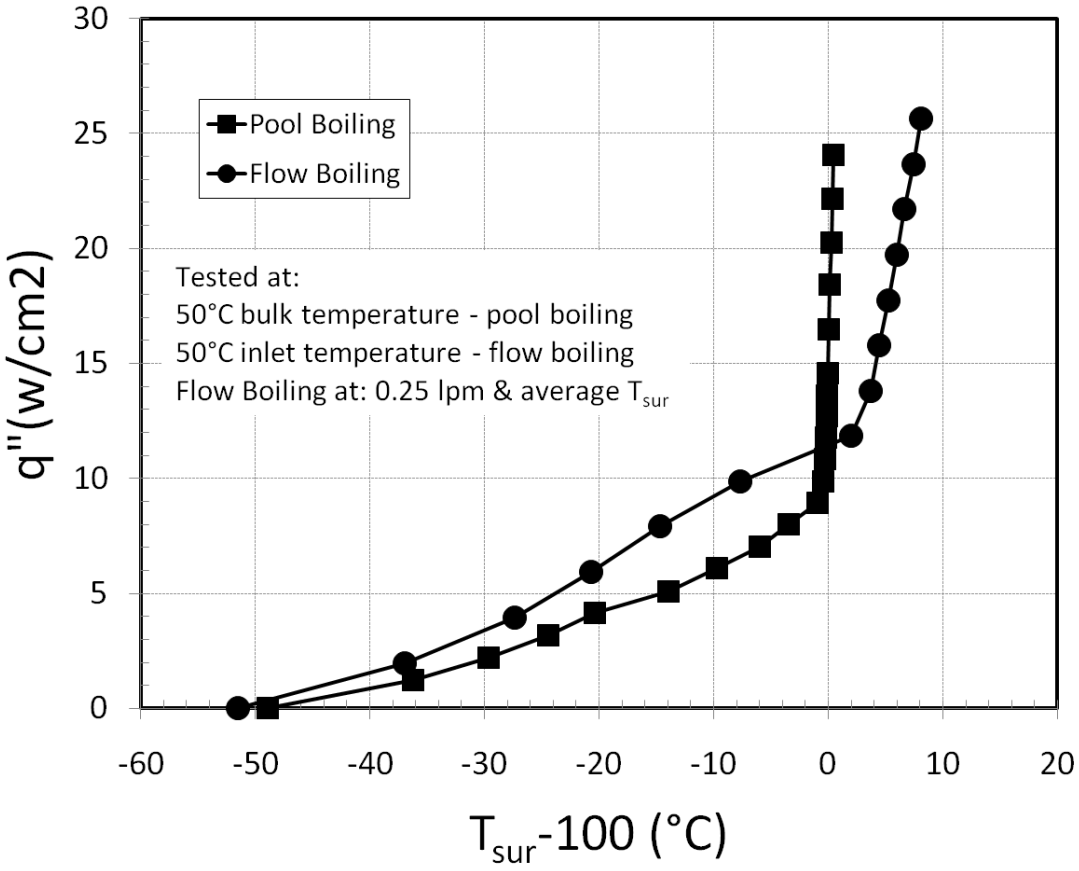

Figure 3.20 Comparison of gassy-subcooled flow boiling to gassy-subcooled pool boiling over coated heaters

3.2.6 Enhancement Through Heater Area Reduction

A benefit of the coating in flow boiling is the potential to reduce the area of the heater and achieve the same heat transfer performance. The possible area reductions can be obtained from the ratio of the heat transfer coefficients between the plain copper heater and the coated heater. For a given $Q/\Delta T$ ratio:

$$\frac{Q}{\Delta T} = h_p * A_p \tag{3.2}$$

$$\frac{Q}{\Delta T} = h_c * A_c \tag{3.3}$$

$$A_c = \frac{h_p A_p}{h_c} \tag{3.4}$$

Equation 3.4 is used to calculate the reduced area of the coated heater. The subscripts p and c represent the plain heater and coated heater respectively.

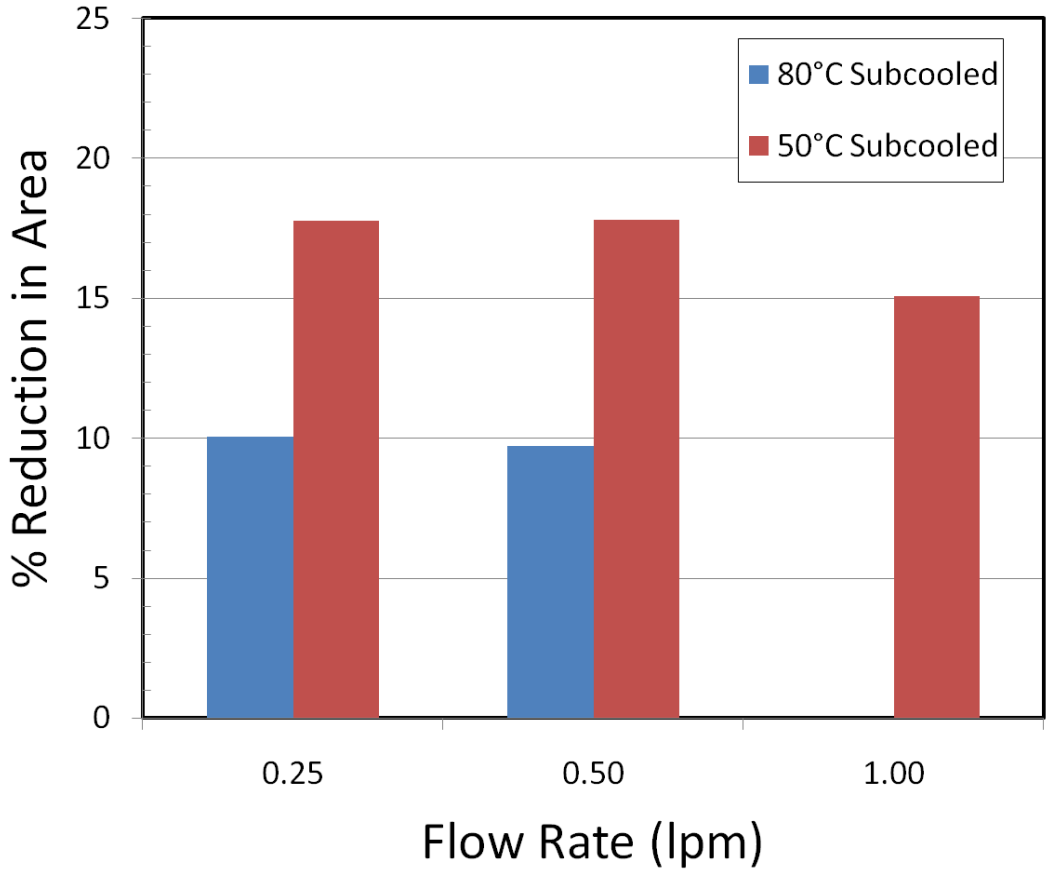

Figure 3.21 Reduction in area

Figure 3.21 shows the percent reduction in area that is possible based on all the tests that reached FDB. The test for 80°C and 1.00lpm was unable to reach FDB due to the limitations in power, and is why the reduction in area is not available and not shown in this figure. The reduction in area was calculated based on the highest heat flux that was reached for both the plain and coated heaters. For example for the 80°C subcooled case at .25lpm, the plain heater reached 26W/cm^2 and the coated heater reached 28W/cm^2 (see Figure 3.16), so the reduction in area was calculated at the highest heat flux that was common to both, 26W/cm^2. It is seen that for 80°C subcooling, the max reduction in area is about 10% and for 50°C subcooling it is about 17.8%. These percentages would increase if the heat flux could be increased with a larger power supply, as suggested by the slope trends in FDB in Figure 3.16 and Figure 3.18.

CHAPTER 4

CONCLUSIONS AND RECOMMENDATIONS

Pool boiling tests were performed under saturated conditions to study the effect of coating thickness on BHT. These tests were performed with coatings of 75µm and 120µm particle sizes and varying thicknesses. An optimal coating thickness was found and it was applied to an extended length flow boiling heater. Flow boiling tests were performed at various flow rates and different subcooling levels. The range of heat fluxes was limited to no more than $30W/cm^2$.

4.1 Pool Boiling

1. The optimal thickness for the coatings of 75µm particle size was 425µm±25µm.
2. The optimal thickness for the coatings of 120µm particle size was 783µm±28µm.
3. Due to the poor bonding of the 120µm particles to the copper substrate, and the very close BHT performance of the two optimal coatings, the 75µm particles at a thickness of 425µm±25µm was chosen for the flow boiling study.

4.2 Flow Boiling

1. Perimeter contamination of the TCMC by a substance which is of significantly lower conductivity than the coating reduces the area for heat flow and increases the heat flux. If the heat flux is not calculated using the actual heat transfer area, which is the area free of contamination, the surface temperatures erroneously appear hotter for the given heat flux. This error is more pronounced in the forced convection part of the flow boiling curve.

2. For both plain and coated surfaces, the presence of noncondensables and flow induced a partially developed boiling regime. Flow rate had as significant an effect on heat transfer as TCMC by enhancing partially developed boiling.
3. Prior to FDB, gas-vapor bubbles accumulated on the heated surfaces, initially as isolated stationary bubbles and eventually blanketing the surfaces with increasing heat flux and with duration of the test. This blanket acted as a thermal resistance layer causing the surface temperatures to increase with increasing heat flux.
4. Below certain heat fluxes, the TCMC proved to be detrimental or to offer no heat transfer enhancement with respect to the plain heater, since in the tests with the TCMC heater, the stationary gas-vapor bubbles were more numerous and started blanketing the heater at lower heat fluxes .
5. For a sufficiently high heat flux, in the FDB regime, TCMC as produced for this study, provided BHT enhancement. This enhancement, in terms of heat transfer area reduction, potentially allowed a reduction of up to ~10% for 80°C subcooling and up to ~17.8% for 50°C subcooling. Greater reductions would be possible with increasing operating power.
6. In terms of surface temperature reduction, TCMC allowed the coated heater to operate between 7 and 10°C cooler than the plain heater at heat fluxes in the FDB region, which can lead to longer life for the heated surface.

4.3 Recommendations

1. Test at higher flow rates to see effect on stationary gas-vapor bubbles. Eventually the bubbles will experience a strong enough drag force to be carried by the flow.
2. Explore other channel geometries, lengths, or orientations of the heater. This study looked at the fundamental flow boiling heat transfer over an extended flat area. In reality, tankless hot water heaters often use round tubes that are positioned in all

orientations. Also, tubes can be much longer than the channel length used by this study.

3. Study the effect of TCMC coatings with regard to flow boiling applications where CHF or dry-out is reached, for example with regard to HVAC applications. The evaporator of an AC system must reach dry-out so only dry vapor flows into the compressor, which is located after the evaporator in the reverse Rankin cycle.

APPENDIX A

PICTORAL ANALYSIS OF STATIONARY BUBBLE PHENOMENON

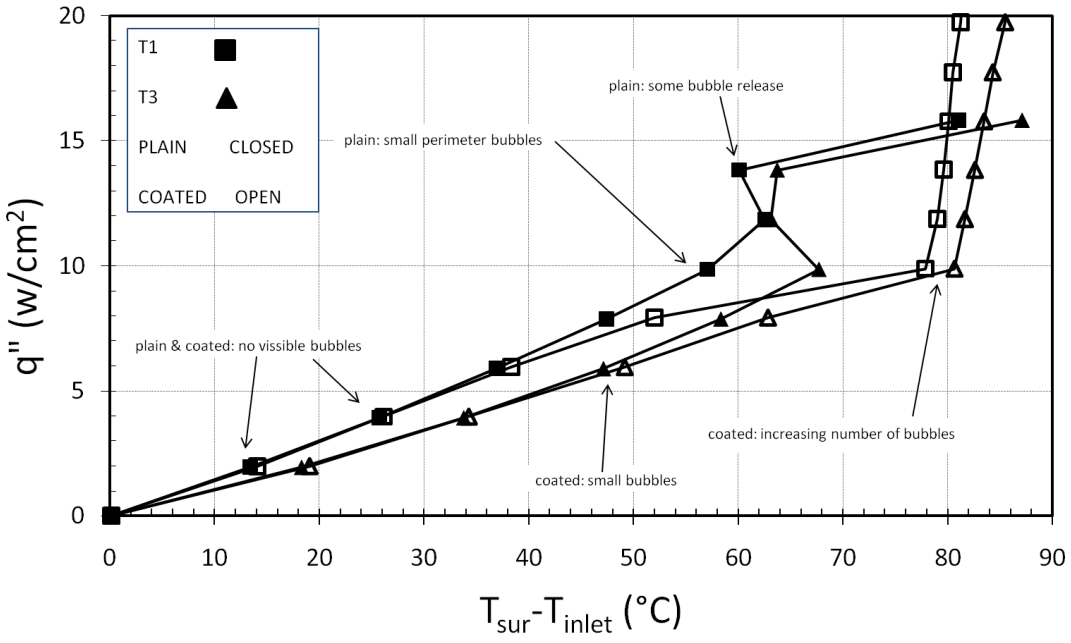

Figure A.1 Flow boiling curves of plain and coated heaters

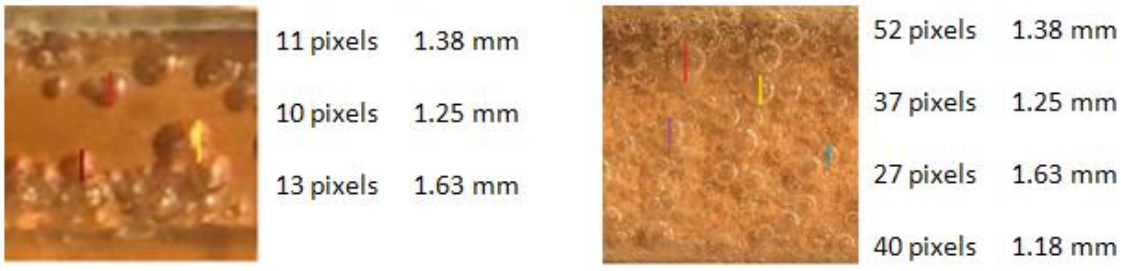

Figure A.2 Number of stationary bubbles over plain heater (left) and over coated heater (right) at 14W/cm^2

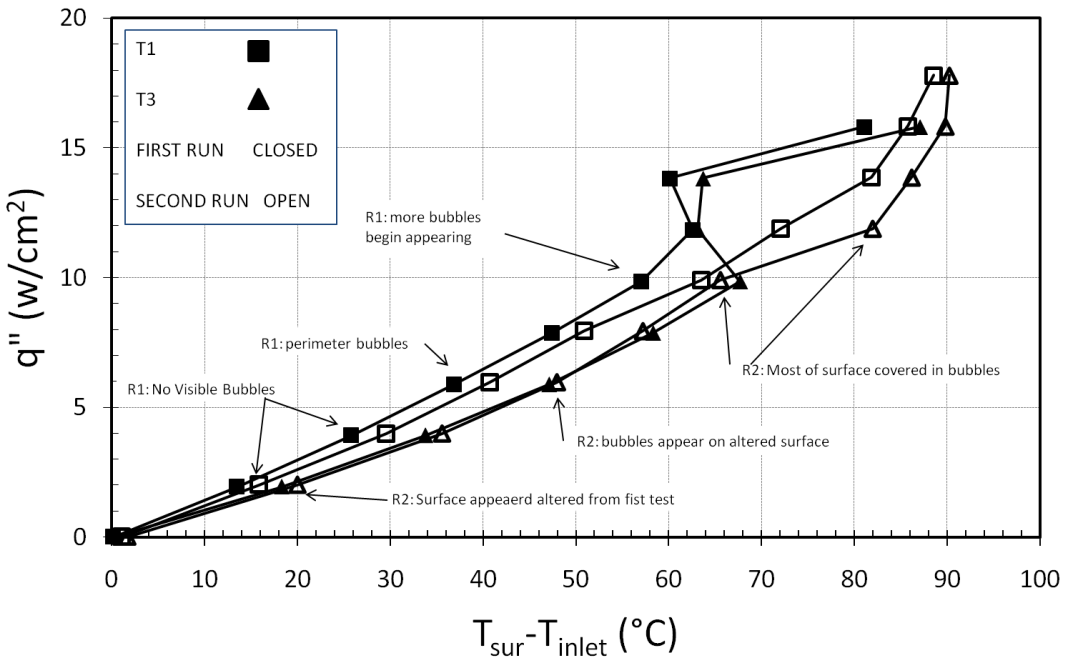

Figure A.3 Flow boiling curves for repeated tests over the same plain heater.

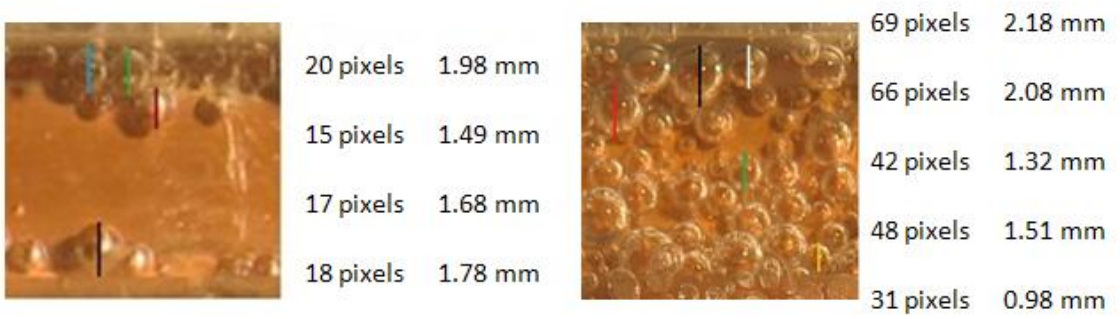

Figure A.4 Number of stationary bubbles of 1st plain heater run (left) and 2nd plain heater run (right) at 12W/cm^2

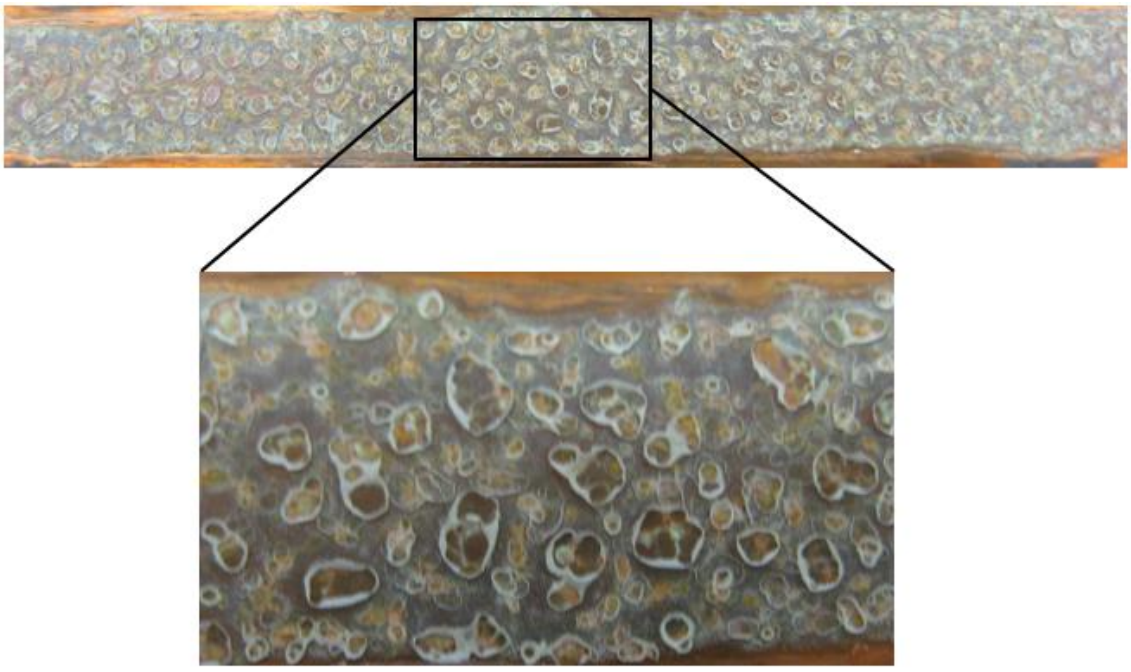

Figure A.5 Fouling on the plain heater after ~10 tests in tap water

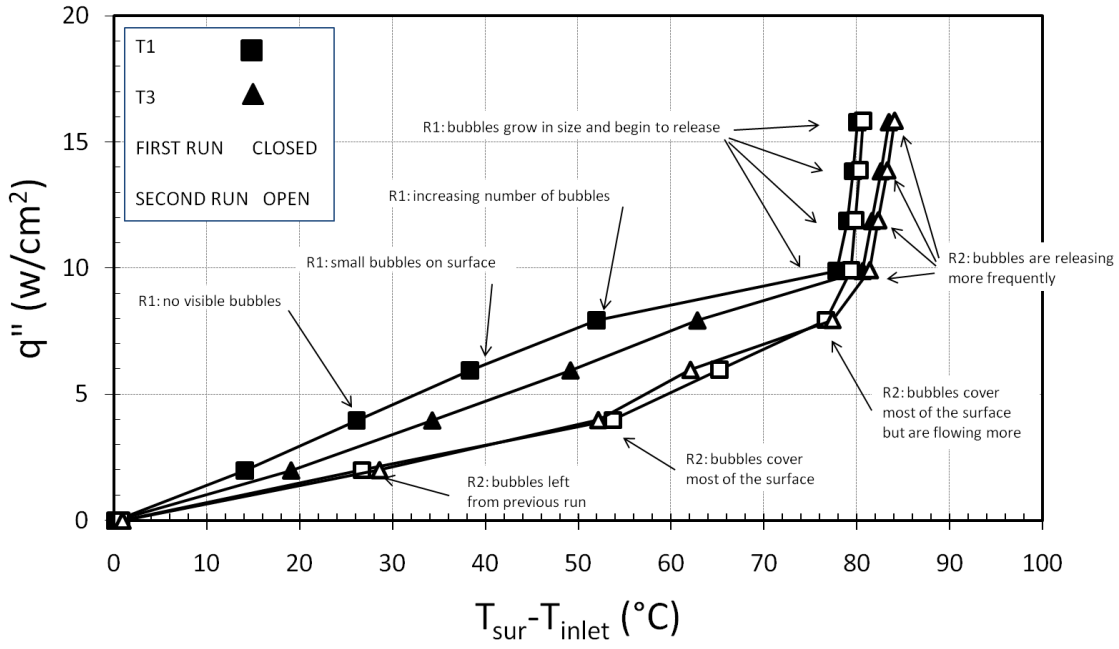

Figure A.6 Flow boiling curve of 1st coated heater run and 2nd coated heater run

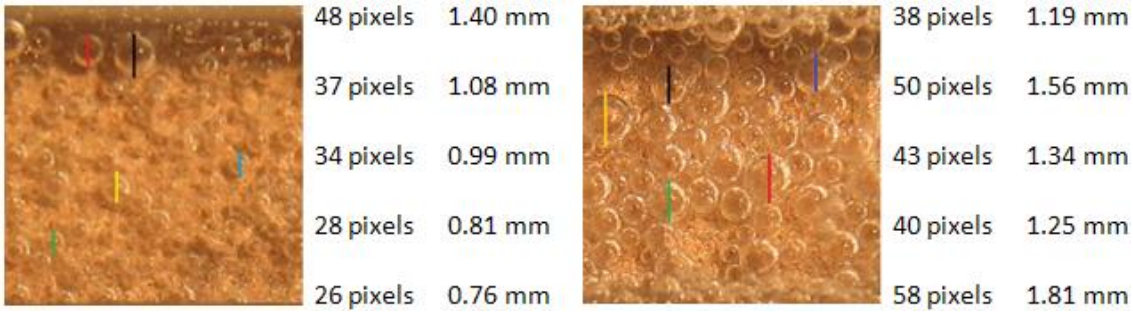

Figure A.7 Number of stationary bubbles of 1st coated heater run (left) and 2nd coated heater run (right) at 12W/cm^2

REFERENCES

[1] Sarwar, M. S., Jeong, Y. H., and Chang, S. H., 2007, "Subcooled Flow Boiling CHF Enhancement with Porous Surface Coatings," International Journal of Heat and Mass Transfer, **50**(17-18) pp. 3649-3657.

[2] Ma, A., Wei, J., Yuan, M., 2009, "Enhanced Flow Boiling Heat Transfer of FC-72 on Micro-Pin-Finned Surfaces," International Journal of Heat and Mass Transfer, **52**(13-14) pp. 2925-2931.

[3] Moreno, G., 2009, "Experimental Investigation of Flow Boiling and Spray Cooling on Enhanced Surfaces in FC-72," **Ph D Dissertation**(The University of Texas at Arlington) pp. Department of Mechanical and Aerospace Engineering.

[4] You, S. M., and Kim, J. H., 2006, "Thermally Conductive Microporous Coating," **US Patent Pending**(20070202321) .

[5] Bergles, A. E., 1997, "Enhancement of Pool Boiling," International Journal of Refrigeration, **20**(8) pp. 545-551.

[6] Cieslinski, J. T., 2002, "Nucleate Pool Boiling on Porous Metallic Coatings," Experimental Thermal and Fluid Science, **25**(7) pp. 557-564.

[7] Das, A. K., Das, P. K., and Saha, P., 2009, "Performance of Different Structured Surfaces in Nucleate Pool Boiling," Applied Thermal Engineering, **29**(17-18) pp. 3643-3653.

[8] Li, C., and Peterson, G. P., 2008, "Experimental Studies on CHF of Pool Boiling on Horizontal Conductive Micro Porous Coated Surfaces," AIP Conference Proceedings, **969**(1) pp. 12-20.

[9] Hsieh, S., and Weng, C., 1997, "Nucleate Pool Boiling from Coated Surfaces in Saturated R-134a and R-407c," International Journal of Heat and Mass Transfer, **40**(3) pp. 519-532.

[10] Kwark, S. M., Kumar, R., Moreno, G., 2010, "Pool Boiling Characteristics of Low Concentration Nanofluids," International Journal of Heat and Mass Transfer, **53**(5-6) pp. 972-981.

[11] Godson, L., Raja, B., Mohan Lal, D., 2010, "Enhancement of Heat Transfer using nanofluids—An Overview," Renewable and Sustainable Energy Reviews, **14**(2) pp. 629-641.

[12] Bang, I. C., and Heung Chang, S., 2005, "Boiling Heat Transfer Performance and Phenomena of Al2O3–water Nano-Fluids from a Plain Surface in a Pool," International Journal of Heat and Mass Transfer, **48**(12) pp. 2407-2419.

[13] You, S.M., Rainey, K.N., and Ammerman, C.N., 2004, "Advances in Heat Transfer,"Elsevier, pp. 73-142.

[14] Chang, J. Y., and You, S. M., 1997, "Enhanced Boiling Heat Transfer from Microporous Surfaces: Effects of a Coating Composition and Method," International Journal of Heat and Mass Transfer, **40**(18) pp. 4449-4460.

[15] Chang, J. Y., and You, S. M., 1997, "Boiling Heat Transfer Phenomena from Microporous and Porous Surfaces in Saturated FC-72," International Journal of Heat and Mass Transfer, **40**(18) pp. 4437-4447.

[16] Thome, J.R., 2004, "Engineering Data Book III," Wolverine Tube, Inc., .

[17] Kakaç, S., and Cao, L., 2009, "Analysis of Convective Two-Phase Flow Instabilities in Vertical and Horizontal in-Tube Boiling Systems," International Journal of Heat and Mass Transfer, **52**(17-18) pp. 3984-3993.

[18] Ganeshan, S., and Rao, M. R., 1982, "Studies on Thermohydraulics of Single- and Multi-Start Spirally Corrugated Tubes for Water and Time-Independent Power Law Fluids," International Journal of Heat and Mass Transfer, **25**(7) pp. 1013-1022.

[19] Krishnamurthy, S., and Peles, Y., 2008, "Flow Boiling of Water in a Circular Staggered Micro-Pin Fin Heat Sink," International Journal of Heat and Mass Transfer, **51**(5-6) pp. 1349-1364.

[20] Qu, W., and Siu-Ho, A., 2009, "Experimental Study of Saturated Flow Boiling Heat Transfer in an Array of Staggered Micro-Pin-Fins," International Journal of Heat and Mass Transfer, **52**(7-8) pp. 1853-1863.

[21] Lee, J., and Mudawar, I., 2009, "Critical Heat Flux for Subcooled Flow Boiling in Micro-Channel Heat Sinks," International Journal of Heat and Mass Transfer, **52**(13-14) pp. 3341-3352.

[22] Wei, J. J., and Honda, H., 2003, "Effects of Fin Geometry on Boiling Heat Transfer from Silicon Chips with Micro-Pin-Fins Immersed in FC-72," International Journal of Heat and Mass Transfer, **46**(21) pp. 4059-4070.

[23] Koşar, A., and Peles, Y., 2006, "Convective Flow of Refrigerant (R-123) Across a Bank of Micro Pin Fins," International Journal of Heat and Mass Transfer, **49**(17-18) pp. 3142-3155.

[24] Kim, J. H., 2006, "Enhancement of Pool Boiling Heat Transfer using Thermally Conductive Microporous Coating Techniques," .

[25] Pivovar, R., 2009, "High Temperature Microporous Coatings: The Effects of Wetting and Wicking on Nucleate Boiling and CHF," .

[26] Kwark, S. M., 2009, "TCMC Evaluation," Internal Document; Micro-Scale Heat Transfer Lab, .

BIOGRAPHICAL INFORMATION

Matthew Mlcak is a native Texan that was born in Wichita Falls, TX and graduated high school from Plano East Senior High School. He attended UT Tyler where he received his B.S. in Mechanical Engineering and graduated Cum Laude. He is currently working on his M.S. in Mechanical Engineering in the Micro Scale Heat Transfer Lab at UT Arlington. After graduating he will be pursuing a career in heat transfer and mechanical engineering. He will also be pursuing his MBA after beginning his career path.